Universita Karlova v Praze
(Charles University in Prague)
Department of Inorganic Chemistry

Coordination Compounds for Medicinal Applications.
Koordinační sloučeniny pro aplikace v medicíně.

Ivan Lukeš

Coordination compounds

Metal – ligand bond

Magnetic Resonance Imaging MRI

Complexation of Radinuclides

2005

23 milions MR examinations in US (25 %)

In world near 100 milions examinations

Contrast agents are used for more than 35 % Examinations

Principles of NMR and MRI

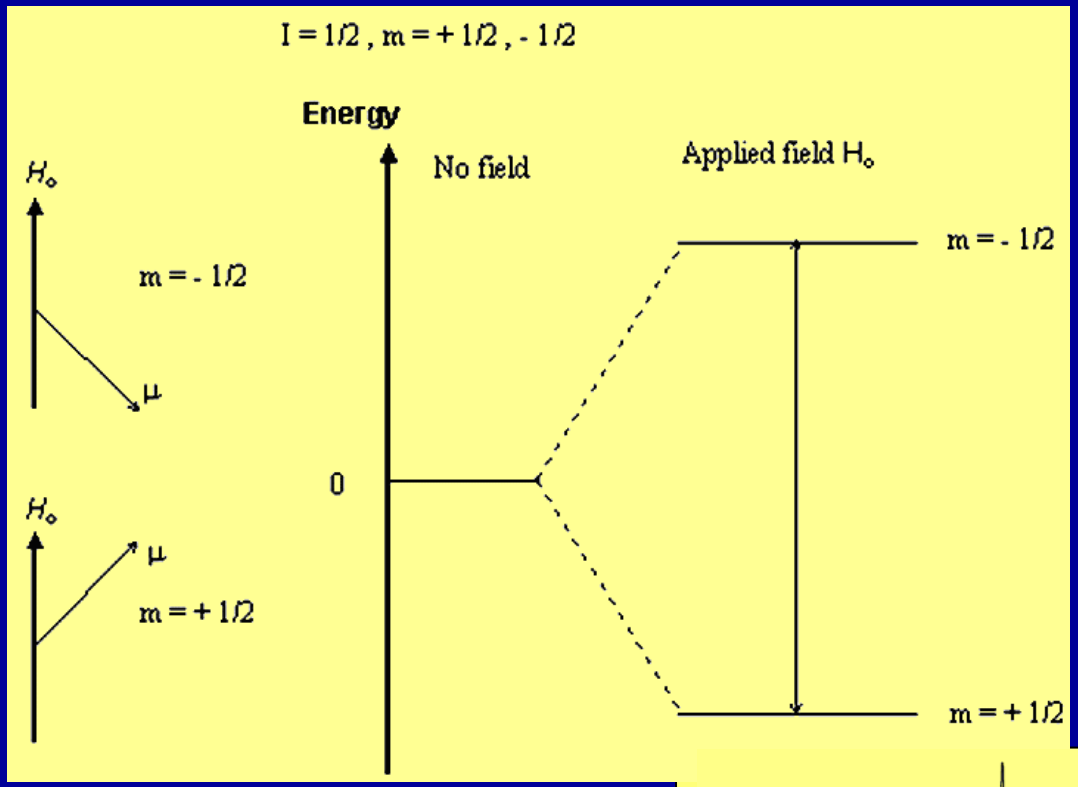

NMR – variable frequency
– positions of peaks

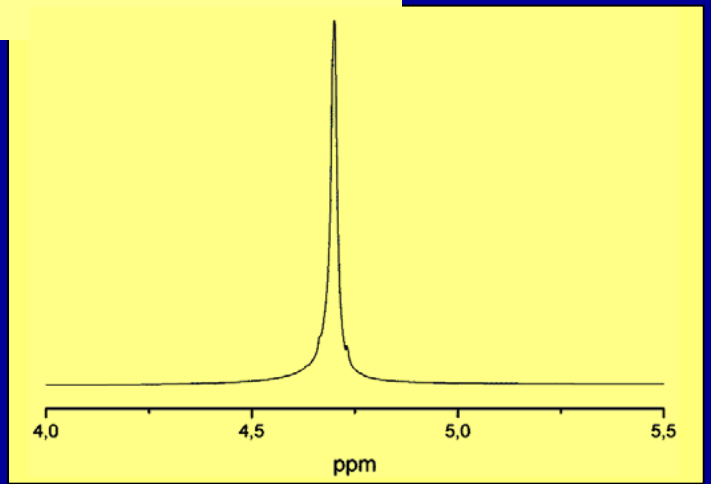

Principles of MRI

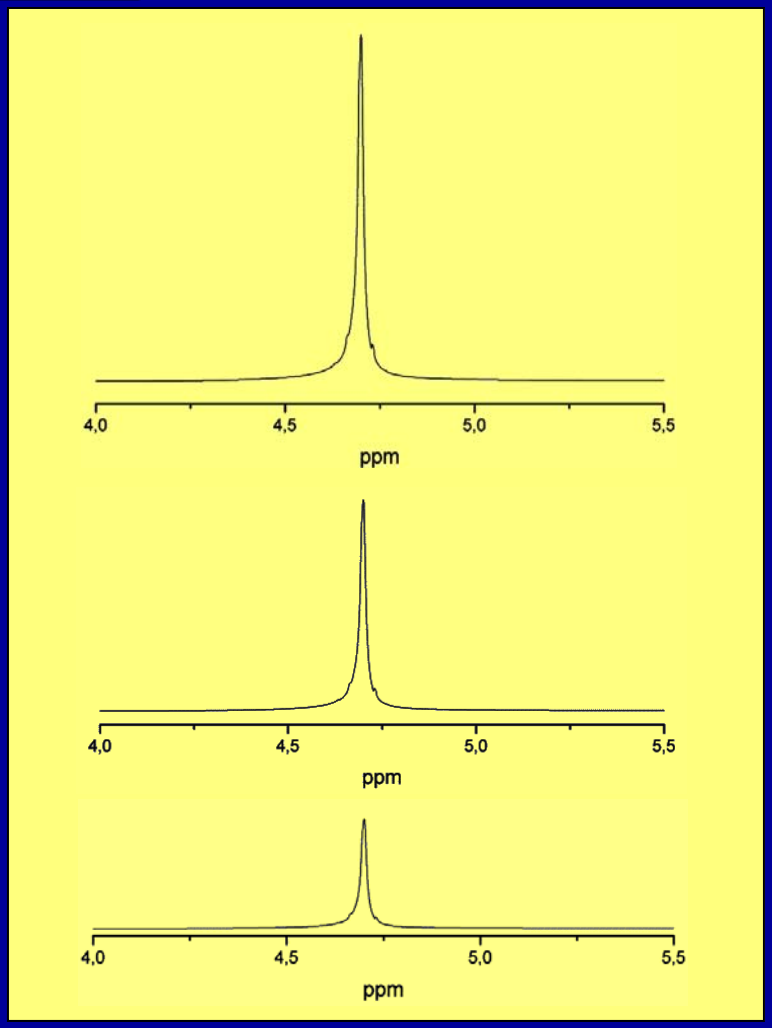

MRI – intensity of peak (water protons)+
spatial resolution – field gradient

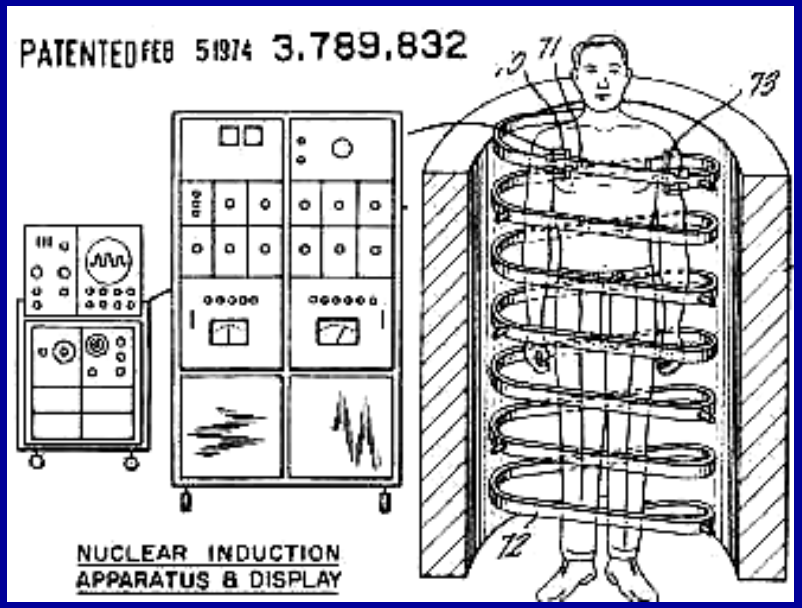

The figure was adopted from U. S. patent ‘832 of Dr. R. Damadian on 3D MRI scanner. The patent was filled on March 17, 1972.

P.C. Lauterbur, P. Mansfield (Nobel Prize 2003),
R. Ernst (1991)
Discrete Fourier Transormation

Principles of MRI

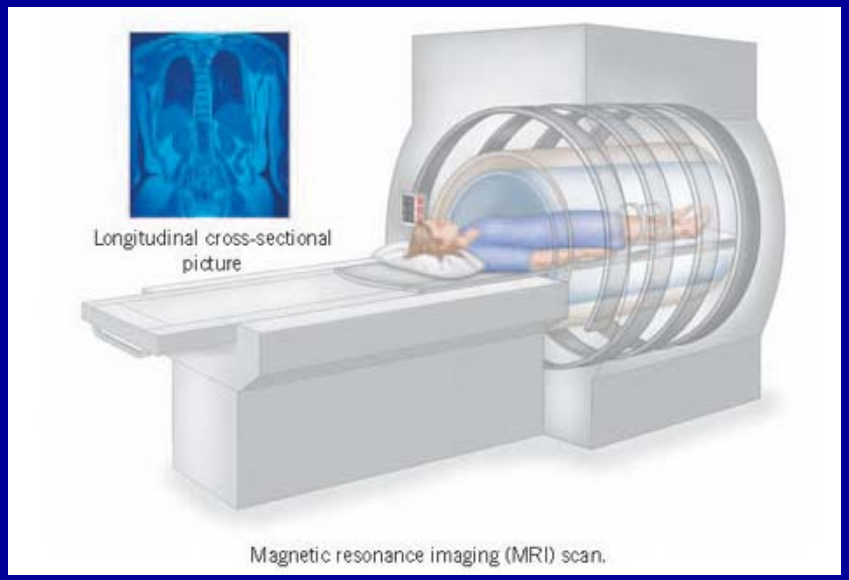

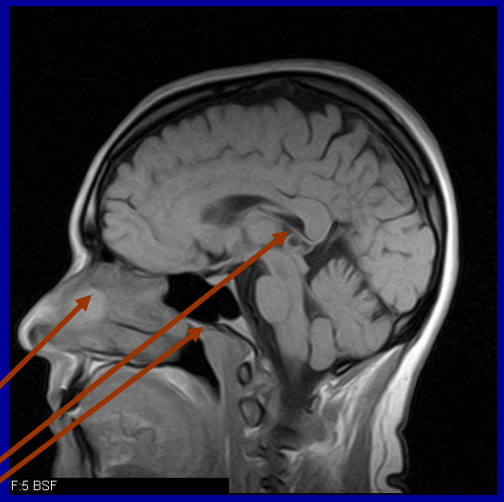

Contrast in MRI originaters from different water concentration among different types of tissue and also from different relaxation rates of water protons

Proton longitudinal T_1

Proton transversal T_2

magnetic relaxation times

T_1 – positive contrast, T_2 – negative contrast

Contrast agents for MRI diagnostics

Proton longitudinal T_1 – paramagnetic species

Proton transversal T_2 – ferromagnetic species

Contrast agents are used for more than 35 % examinations

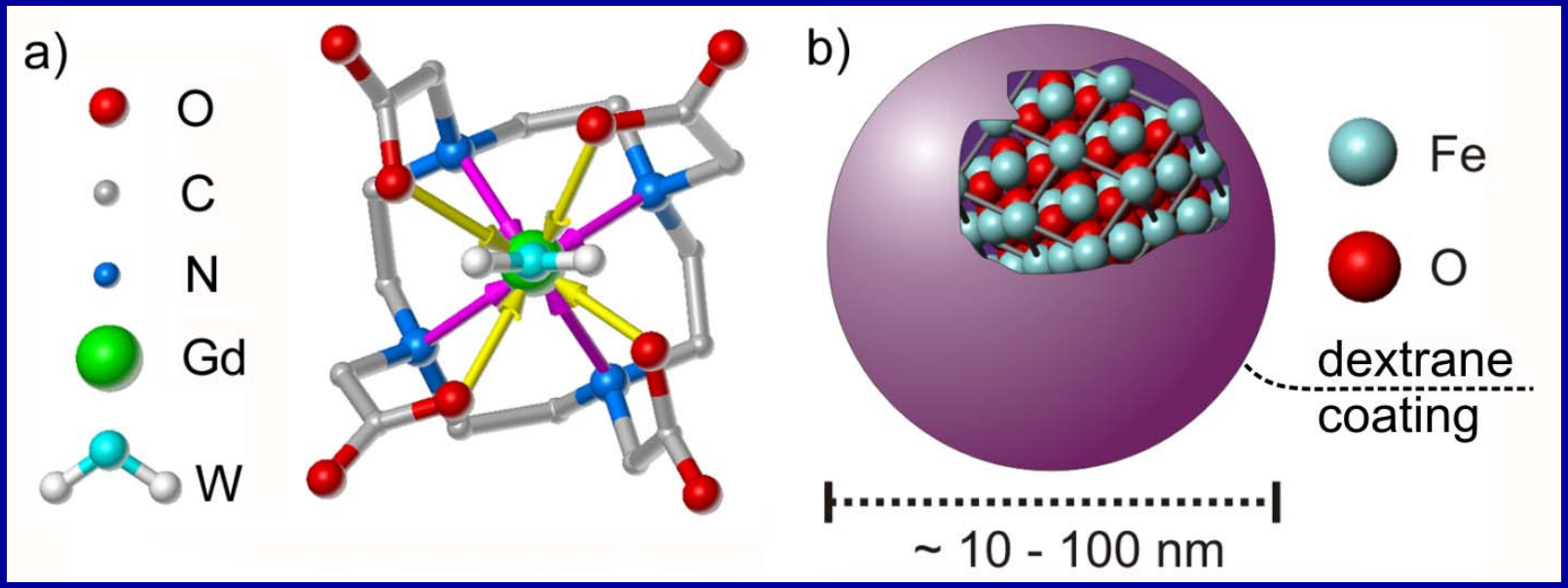

95 % CAs are based on Gd(III)

Contrast agents for MRI diagnostics

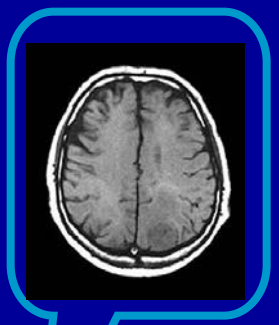

Without CA

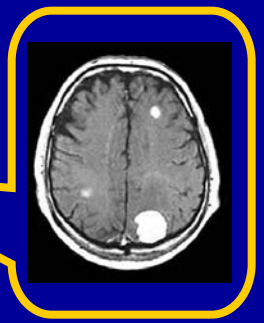

With extracelular Gd(III) CA

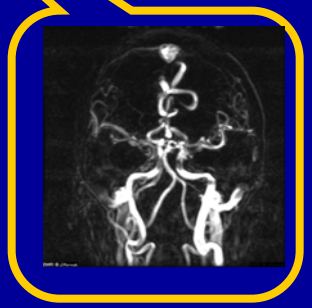

With angiographical Gd(III) CA

Interaction of the water molecules with the gadolinium(III) complex

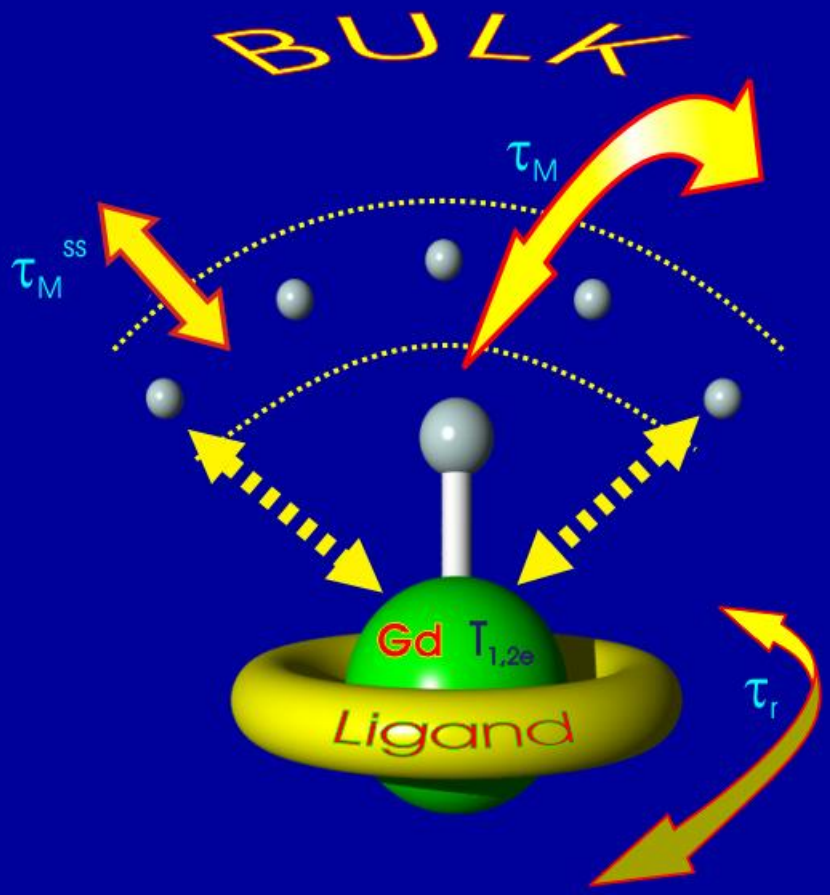

Efficiency of contrast agent is expressed as *relaxivity*, r_1.

r_1 ~ ability of 1mM CA solution to increase of longitudial relaxation rate ($1/T_1$)

$$r_1 = f(q, \tau_M, \tau_R, \tau_M^{SS}, T_{1,2e})$$

Theoretical profile of relaxivity at 20 MHz, 37 °C

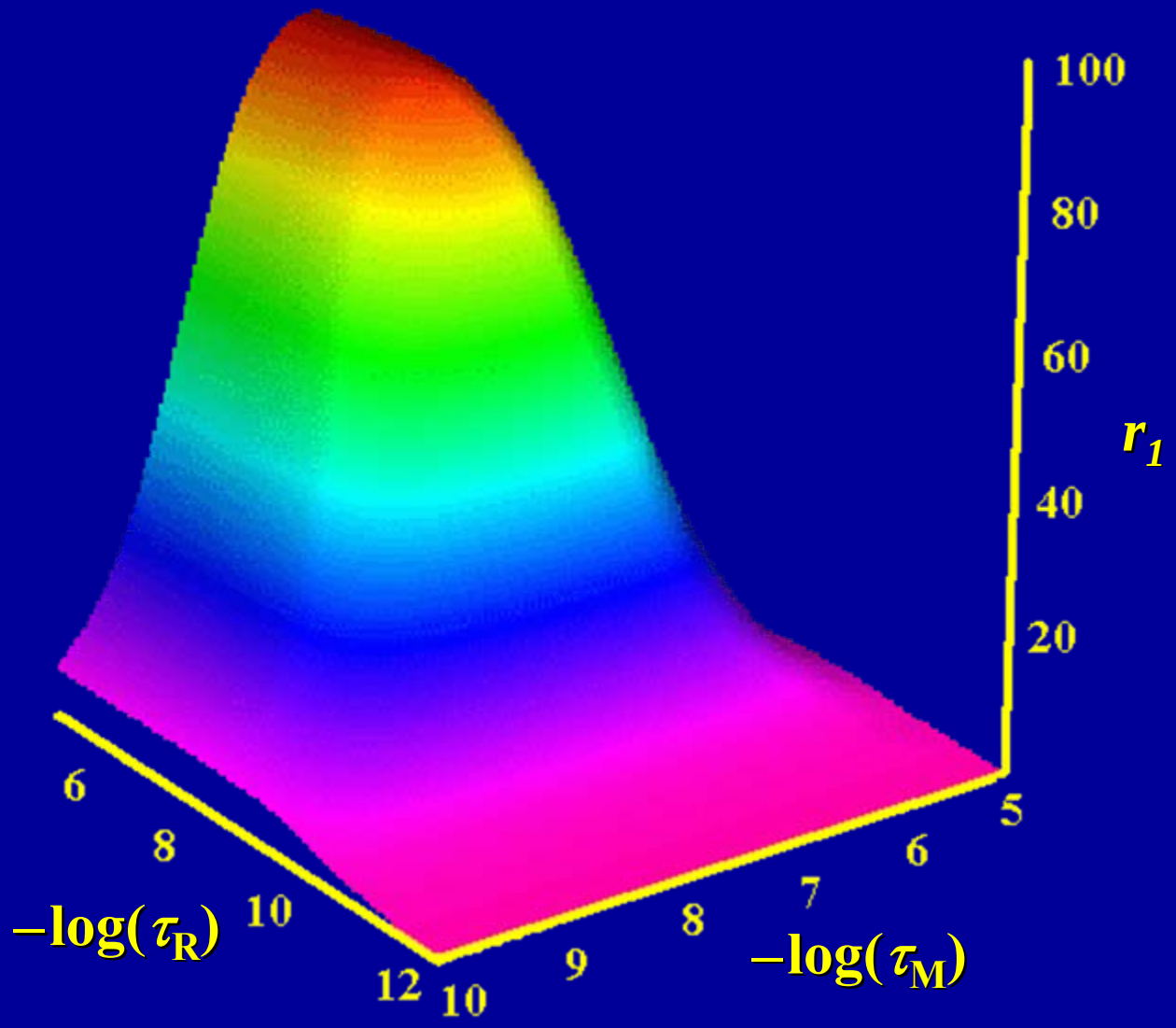

Simulations of relaxivity as a function of proton Larmor frequency

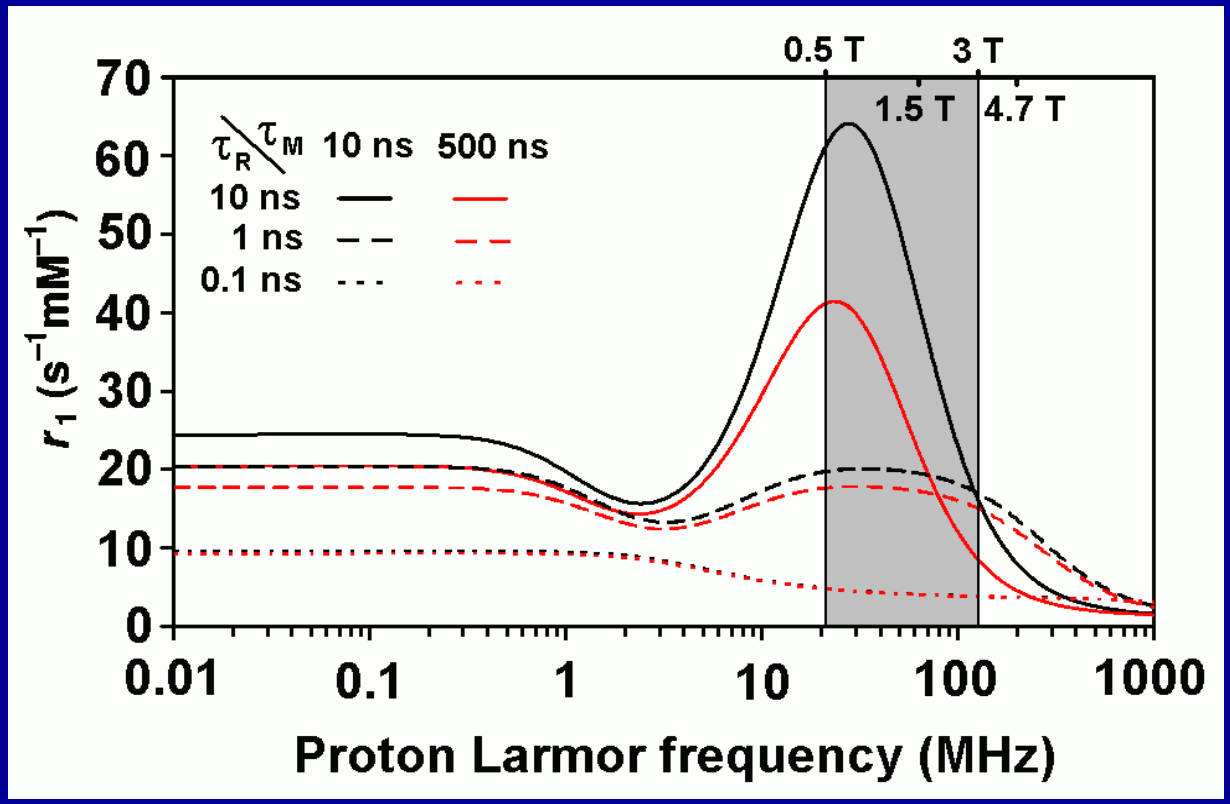

(¹H NMRD profile) T = 37 °C, $^{298}\tau_v$ = 40 ps, $\Delta^2 = 10^{19}$ s^{-2}, R_{GdH} = 3.1 Å.

The gray area shows the range of imaging fields currently used in clinics.

Ligads for MRI utilizations

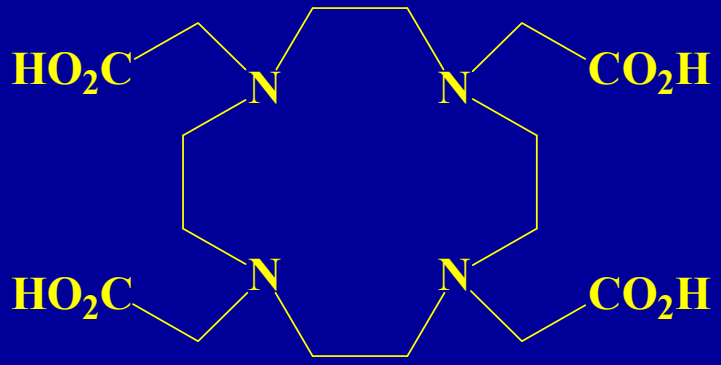

H_4dota

Dotarem®, ProHance®, Gadovist®

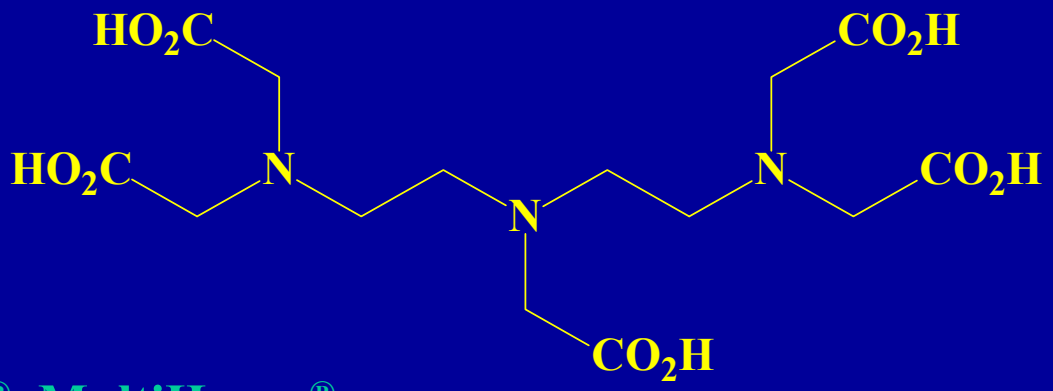

H_5dtpa

Magnevist®, Omniscan®, MultiHance®
OptiMARK®, Eovist®, AngioMARK®

Structures of the Complexes

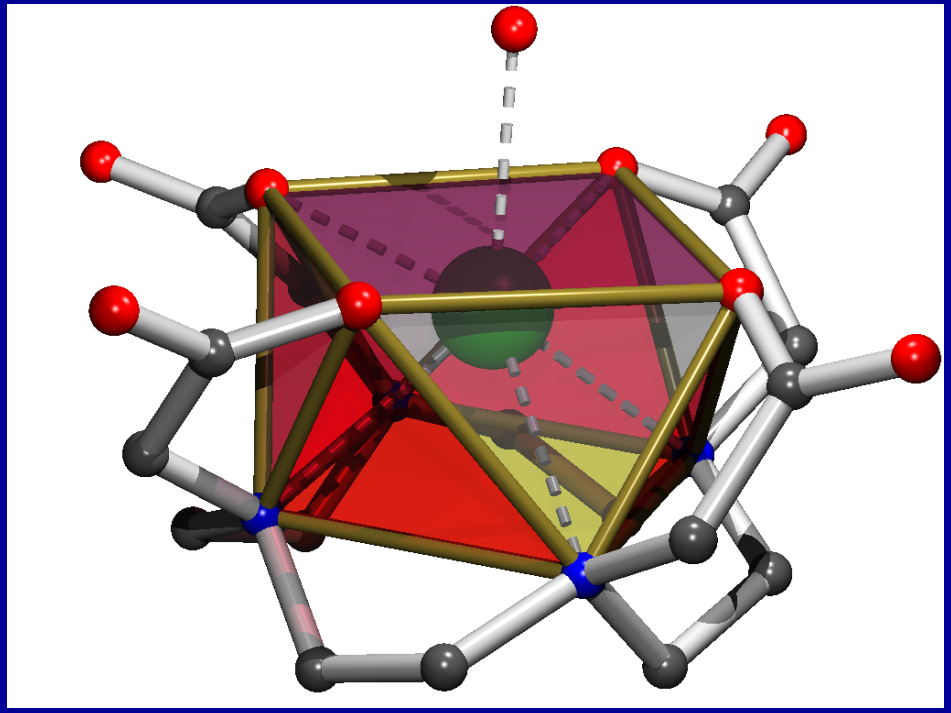

$[Gd(dota)]^-$

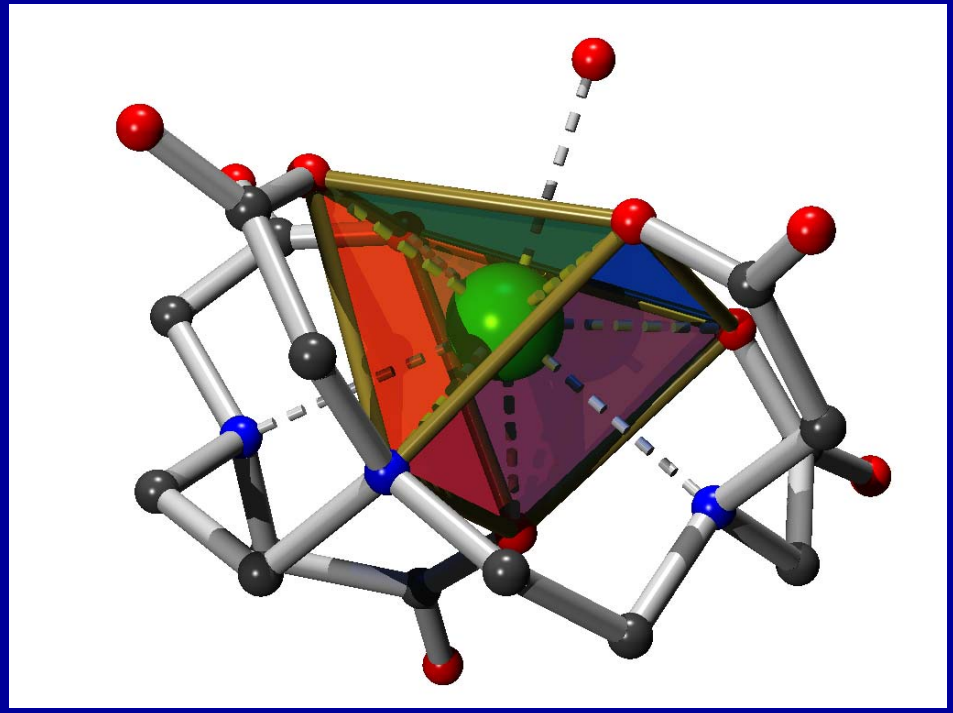

$[Gd(dtpa)]^{2-}$

$$r_1 = f(q, \tau_M, \tau_R, \tau_M^{SS}, T_{1,2e})$$

Bifunctional phosphinic acid derivatives with optimal τ_M 10 – 40 ns

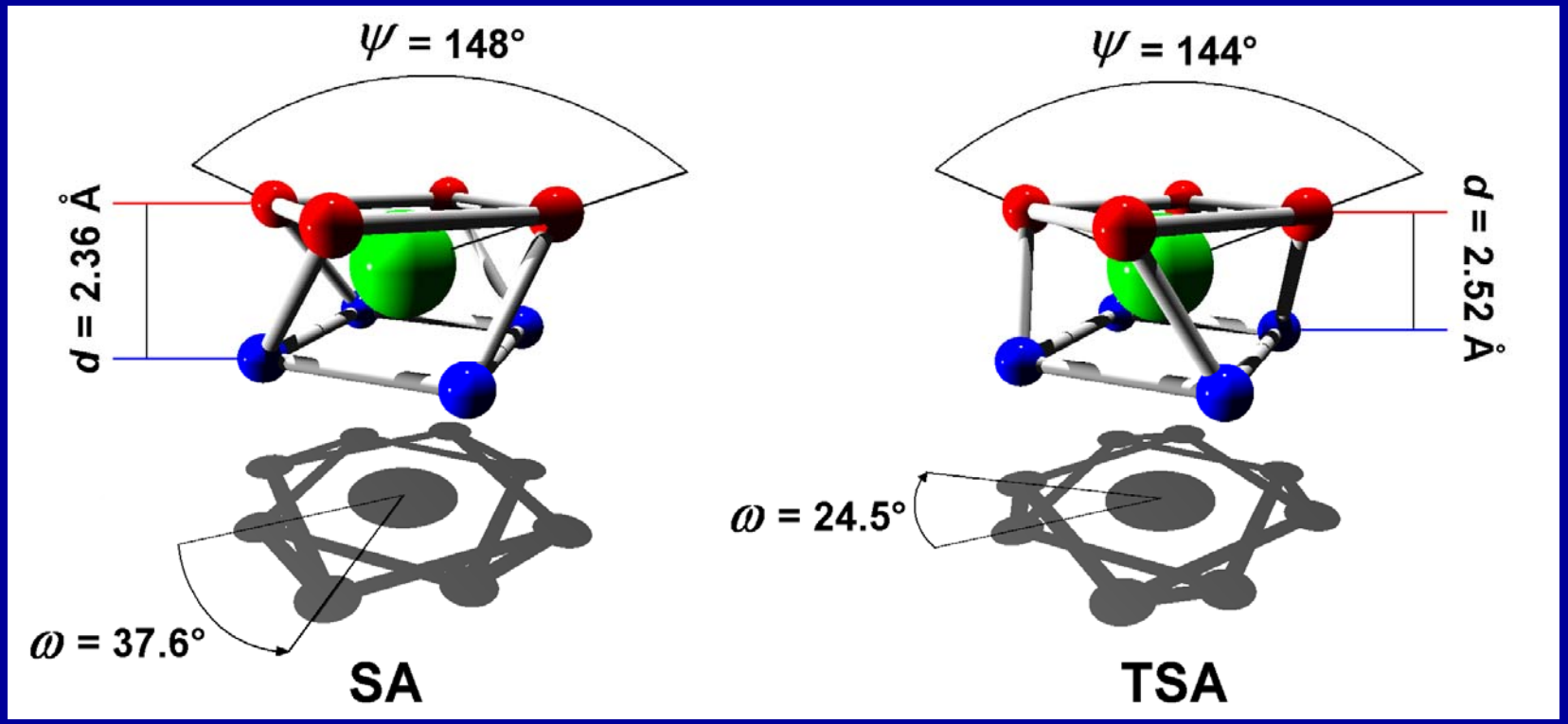

I. Lukeš, J. Kotek, P. Vojtíšek, P. Hermann: *Coord. Chem. Review*, 2001, 216, 287-312

P. Vojtíšek, P. Cígler, J. Kotek, J. Rudovský, P. Hermann, I. Lukeš: *Inorg. Chem.*, 2005, 44, 5591-9

J. Kotek, J. Rudovský, P. Hermann, I. Lukeš: *Inorg. Chem.*, 2006, 45, 3097-3102

P. Hermann, J. Kotek, V. Kubíček, I. Lukeš : *Dalton Trans.*, 2008, 3027-47

Bifunctional phosphinic acid derivatives with optimal τ_M 10 – 40 ns

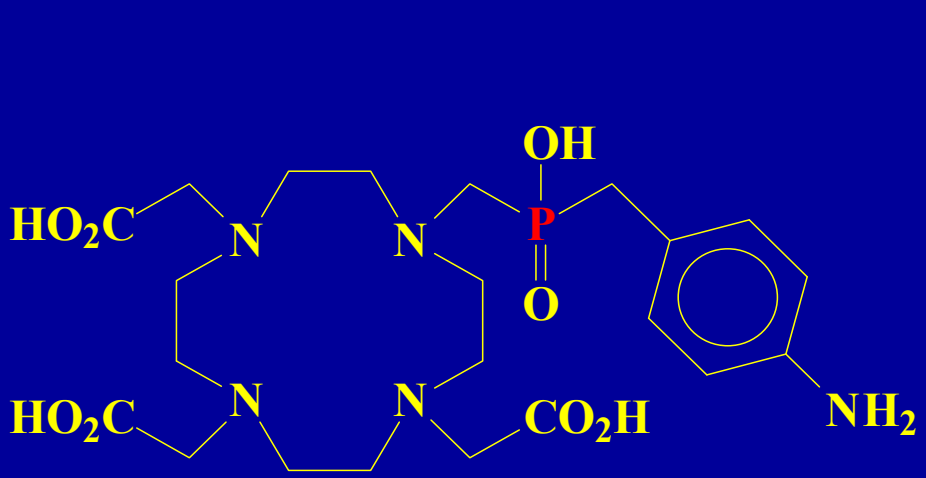

H_4do3aP^{ABn}

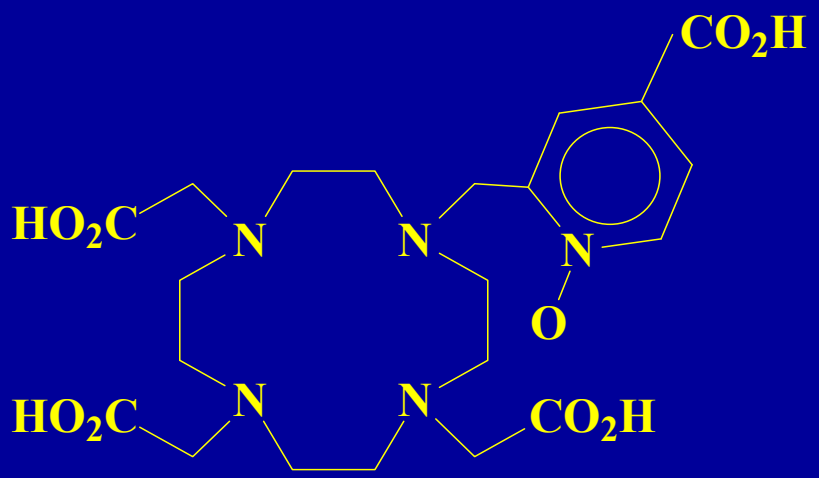

$H_3do3a\text{-}py^{NO\text{-}C}$

suitable for conjugation of MRI contrast agent to macromolecule

J. Rudovský, J. Kotek, P. Hermann, I. Lukeš, V. Mainero, S. Aime: *Org. Biomol. Chem.*, 2005, 3, 112

M. Polášek, J. Rudovský, P. Hermann, I. Lukeš, L.V. Elst, R.N. Muller: *Chem. Comm.*, 2004, 2602

M. Polášek, M. Šedinová, J. Kotek, L.V. Elst, R.N. Muller, P. Hermann, I. Lukeš: *Inorg. Chem.*, 2009, 48, 455-465

M. Polášek, J. Kotek, P. Hermann, I. Císařová, K. Binneman, I. Lukeš: *Inorg. Chem.*, 2009, 48, 466-475

$$r_1 = f(q, \tau_M, \tau_R, \tau_M^{SS}, T_{1,2e})$$

The chemical/physical features that affect τ_R

Slow molecular tumbling

Immobilization of low-molecular Gd(III) complexes

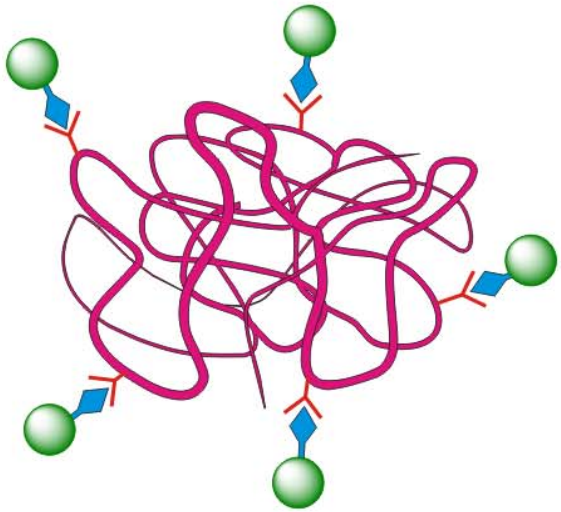

non-covalent protein adduct

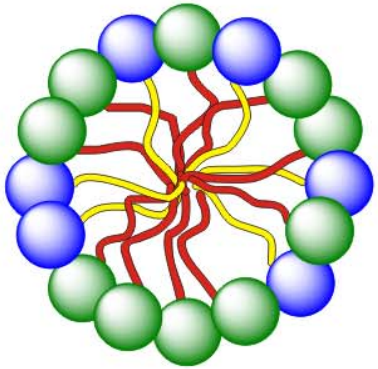

combined micelle

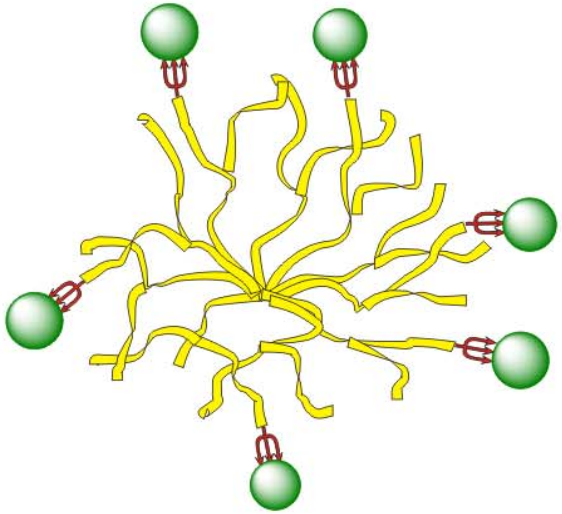

covalent dendrimeric conjugate

Covalent – linear carrier, spheric carrier

Conjugation with PAMAM

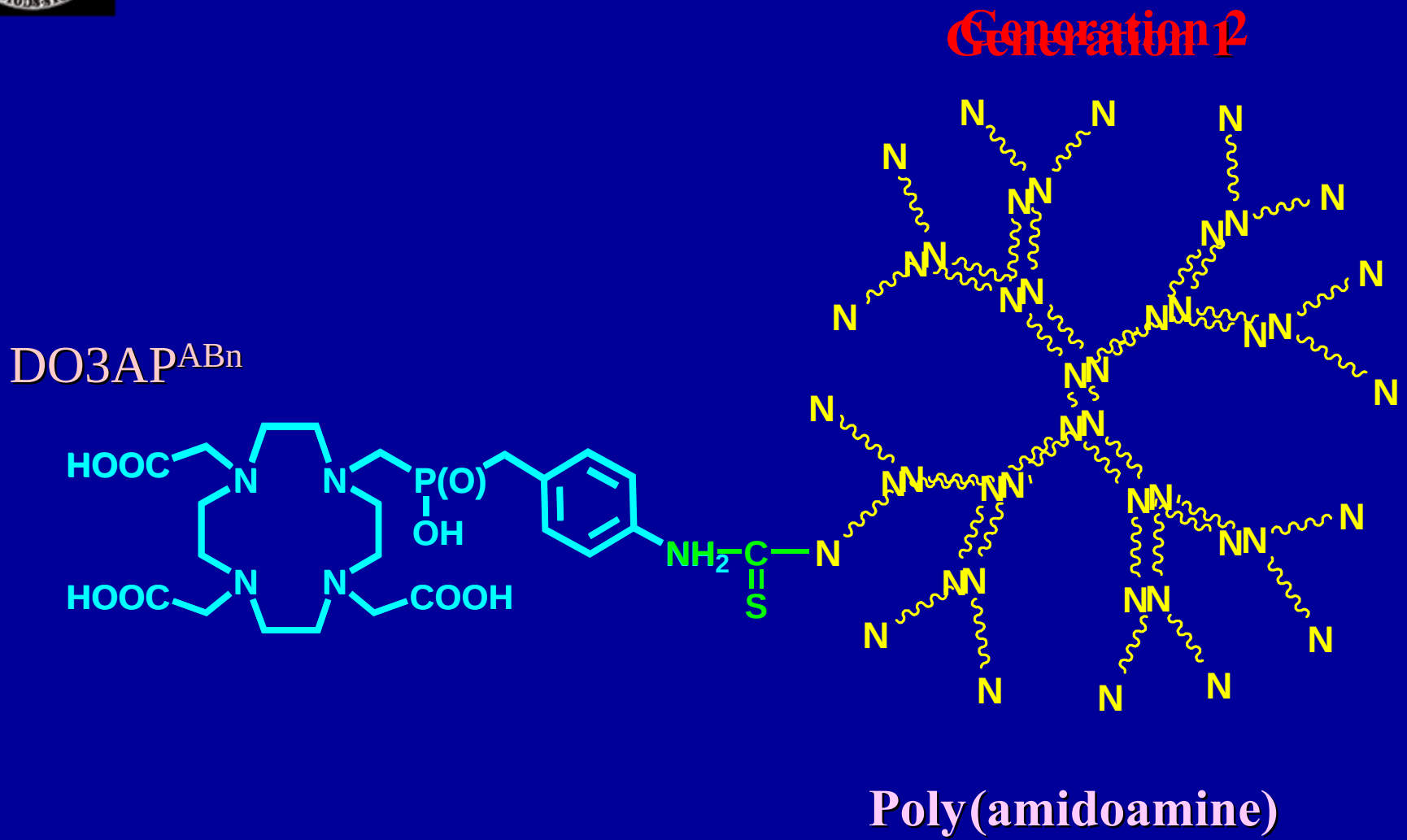

J. Rudovský, P. Hermann, M. Botta, S. Aime, I. Lukeš: *Chem. Comumun.*, 2005, 2390
J. Rudovský, M. Botta, P. Hermann, K.I. Hardcastle, I. Lukeš, S. Aime: *Bioconjgate Chem.*, 2006, *17*, 975

^{1}H NMRD profiles

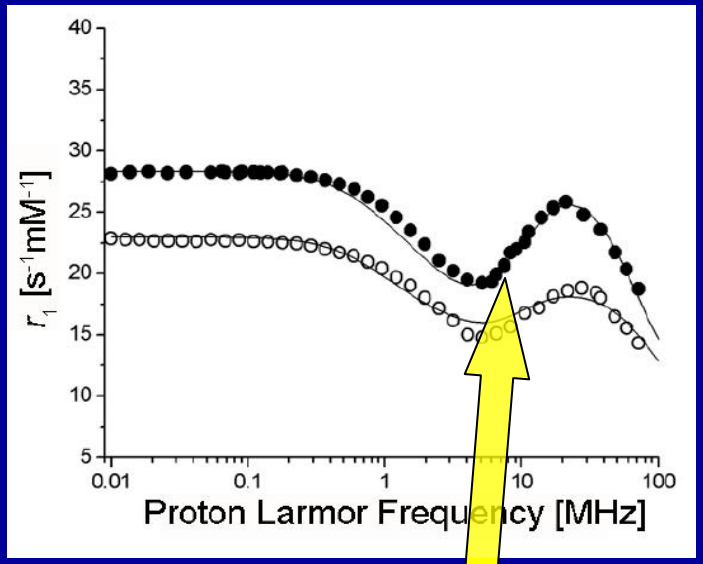

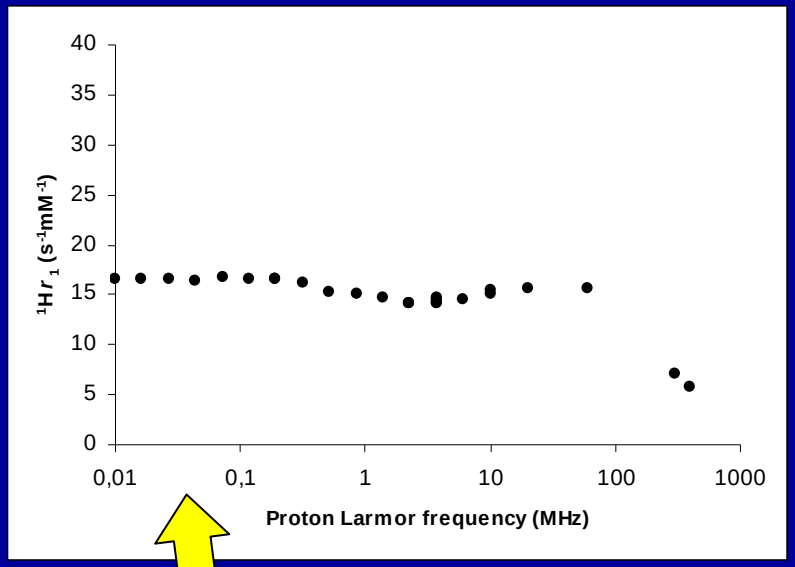

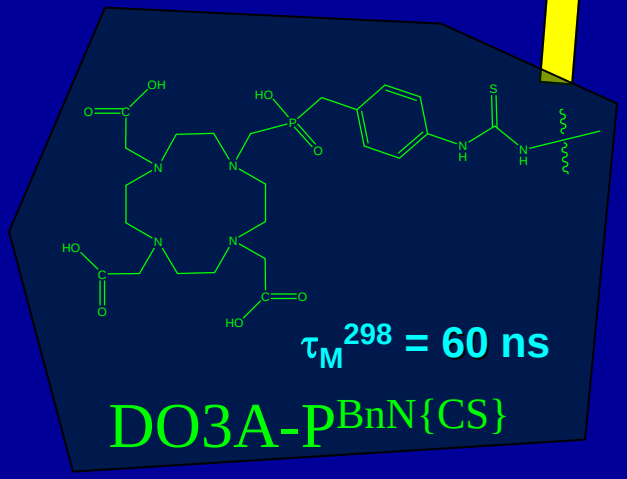

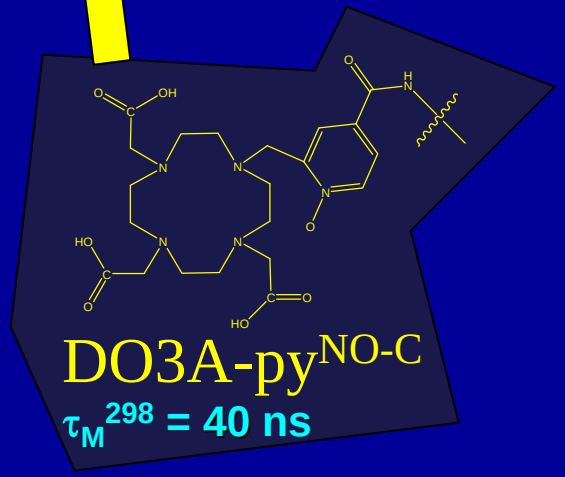

M. Polášek, P. Hermann, J.A.Peters, C.G.G.C. Geraldes, I. Lukeš: *Bioconjgate Chem., in press*

J. Rudovský, M. Botta, P. Hermann, K.I. Hardcastle, I. Lukeš, S. Aime: *Bioconjgate Chem.*, 2006, *17*, 975

Theoretical and experimental relaxivities as a function of τ_r

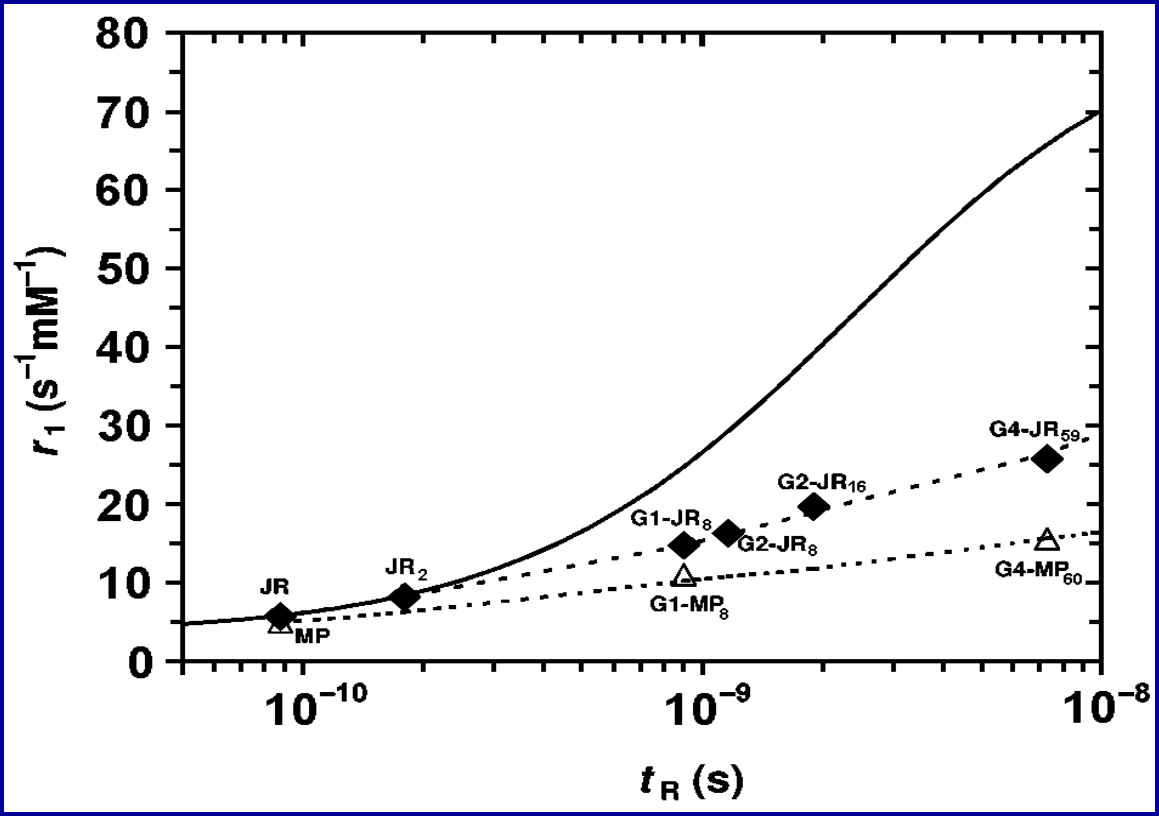

Experimental relaxivities (20 MHz, 25 °C) as a function of theoretical τ_R for G*n*–PAMAM–$[Gd(do3aP^{ABn})(H_2O)]_x$ (full diamonds, G*n*–JR_x) and –$[Gd(do3apy^{NO\text{-}C})(H_2O)]_y$ (open triangles, G*n*–MP_y) conjugates.

Anchoring of Gd(III) complex on TiO_2 nanoparticles

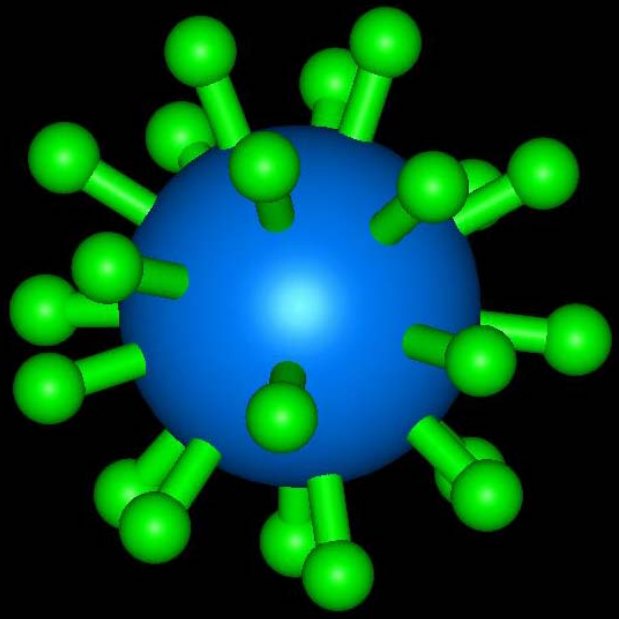

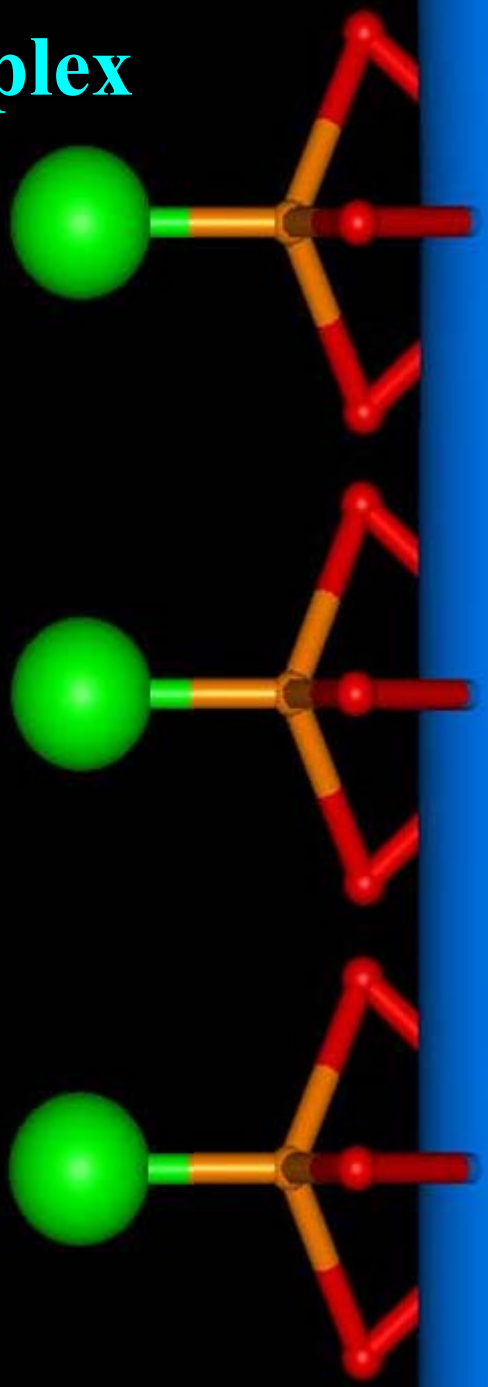

Advantages of our approach:

- No need of working with silylesters
- TiO_2 is highly stable and easily preparable in nanosize
- First complexation, then adsorption
- Formation of monolayer – better surface definition
- Phosphonate adsorbs buch more stable than pyrokatechol

Anchoring of Gd(III) complex with DOTA-like ligand on TiO_2 nanoparticles

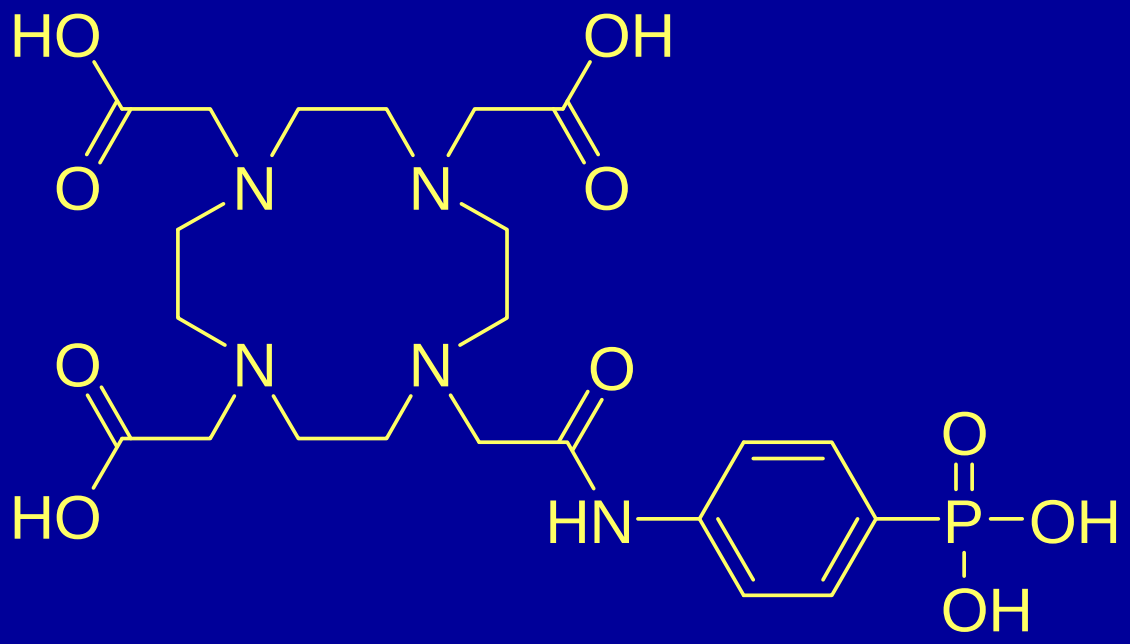

DOTAPP

I. Řehoř, V. Kubíček, J. Kotek, P. Hermann, I. Lukeš, J. Száková, L. Vander Elst, R. N. Muller, J. A. Peters: *J. Materals Chem*., 2009, 19, 1494-1500

Anchoring of Gd(III) complex on the TiO_2 surface

TiO_2 – Degussa (type P25, diameter 30 nm, specific surface ~ 50 m^2/g)

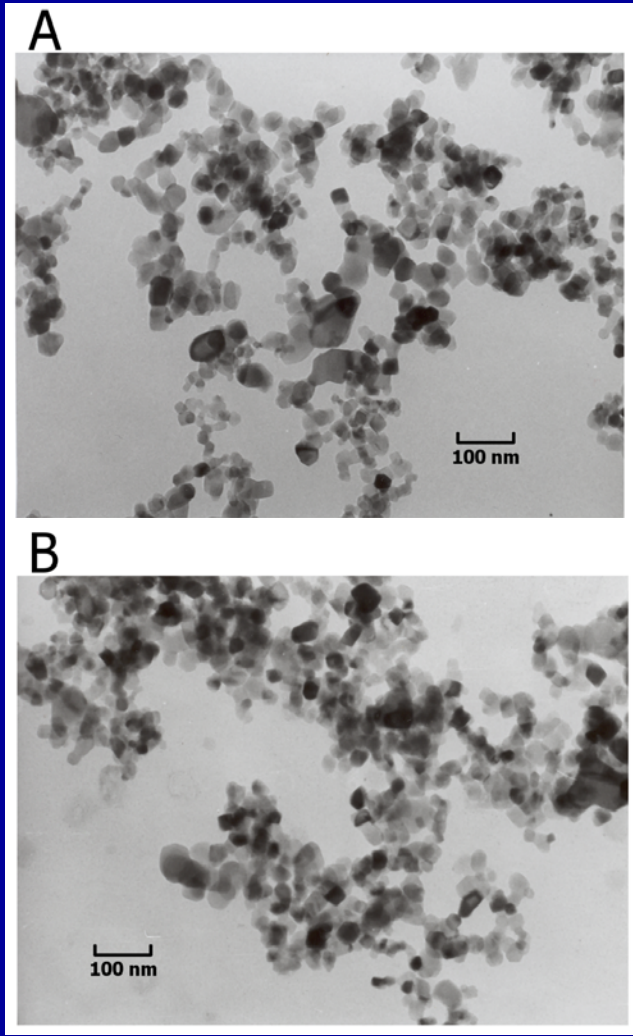

TiO_2 in H_2O and the suspension was sonificated in an ultrasonic bath for 20 min. Then, a solution of a Ln(III) DOTAPP complex 2 in H_2O was added. The pH of the obtained suspension was adjusted to 3.5 and then it was stirred at 70 °C for 3 days followed by 4 h of cooling down.
The resulting suspension was washed with water and concentrated on ultrafiltration cell six times.

Qquantified by ICP-AES:
The content of TiO_2 was 10.0 g/L
the adsorbed amount of the Ln(III)-DOTAPP complex was 52 μmol/g TiO_2.
Surface is fully covered.

NMRD profiles of Gd(III)-DOTAPP

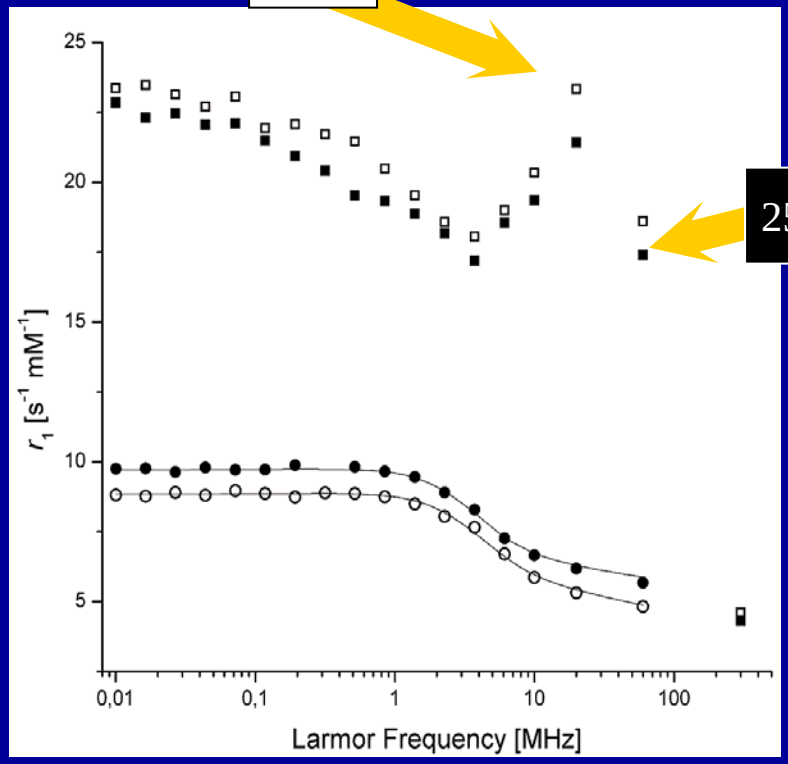

Due to the uncommon shape of the NMRD profile an evaluation of the parameters by fitting the profile was not possible.

An NMRD profile, simulated using a τ_{RH} value of 3 ms (from the Debye-Stokes-Einstein relation for particles 30 nm) and with the other parameters the same as those of free Gd(III)-DOTAPP has a maximum which is of about the same magnitude as that observed for Gd(III)-DOTAPP + TiO_2. This suggests that the Gd(III) chelates are effectively immobilized on the nanoparticles.

The relaxivity of the suspension increases upon increase of the temperature. This confirms that the relaxivity is no longer governed by the rotational correlation time.

Cyclodextrins

as rigid core carrier for middle M_r …

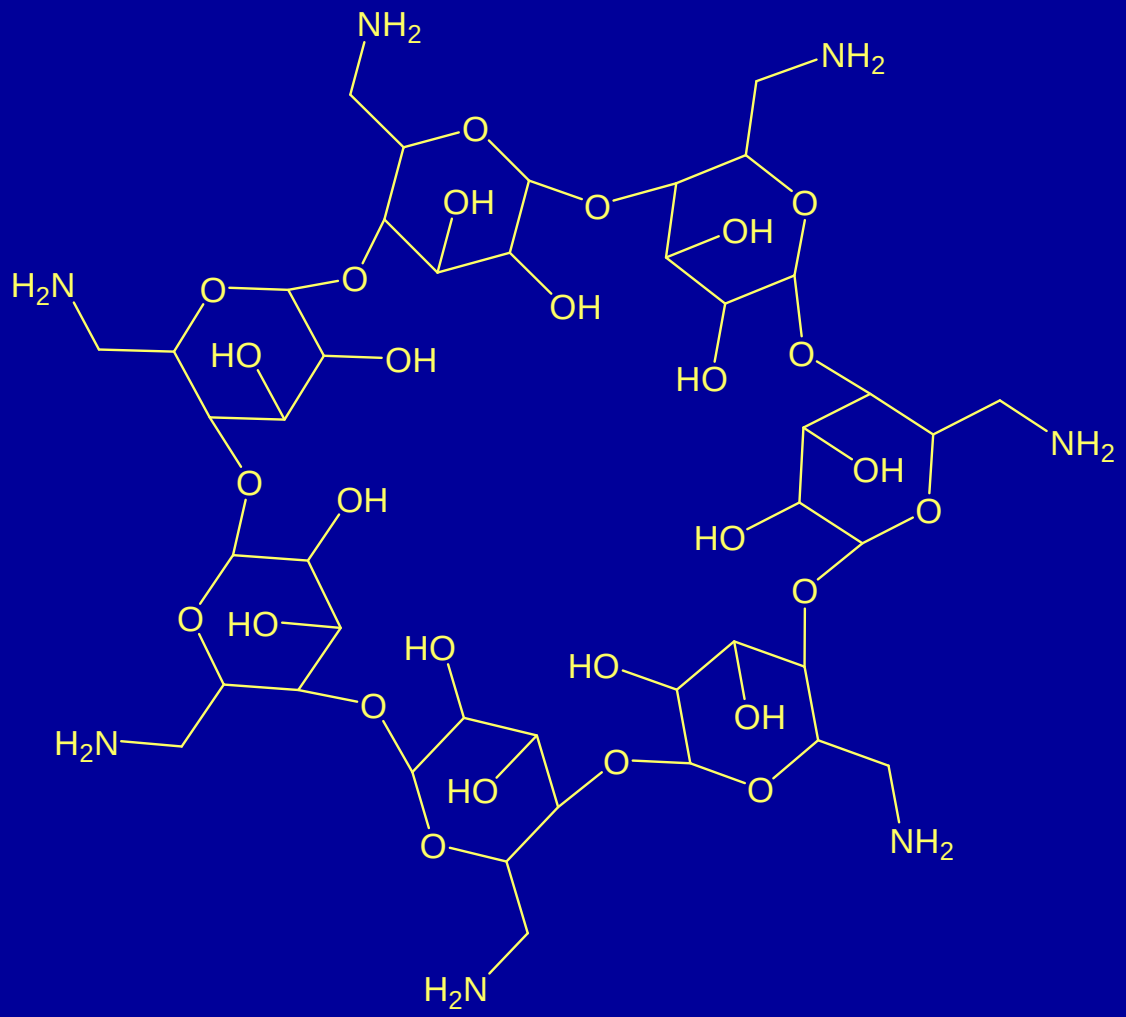

Synthesis of conjugates…

CD-NH_2 + L-NCS

H_2O, pH 8-9

40 °C, 24 h

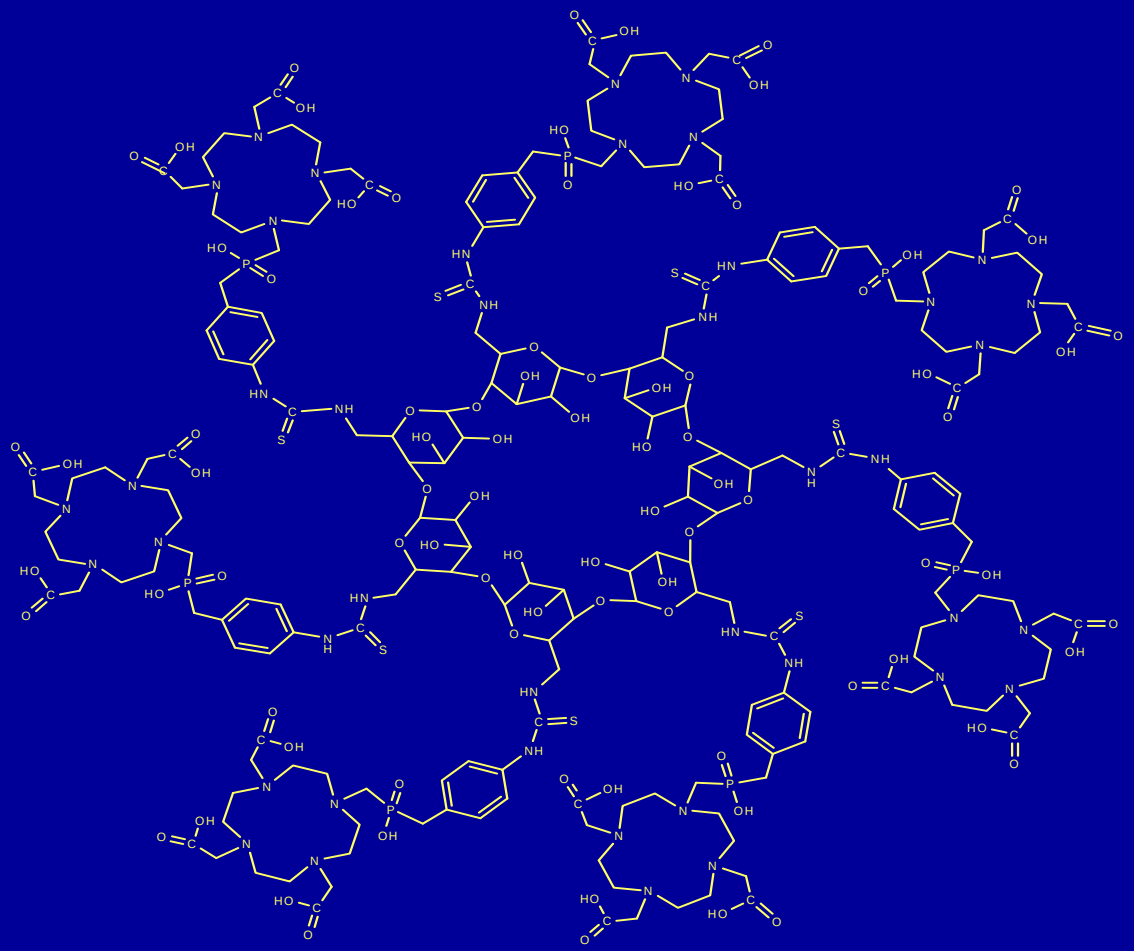

Synthesis of conjugates…

CD-NH_2 + L-*COOH*

Peptide coupling: ligand –COOH to dendrimer –NH_2

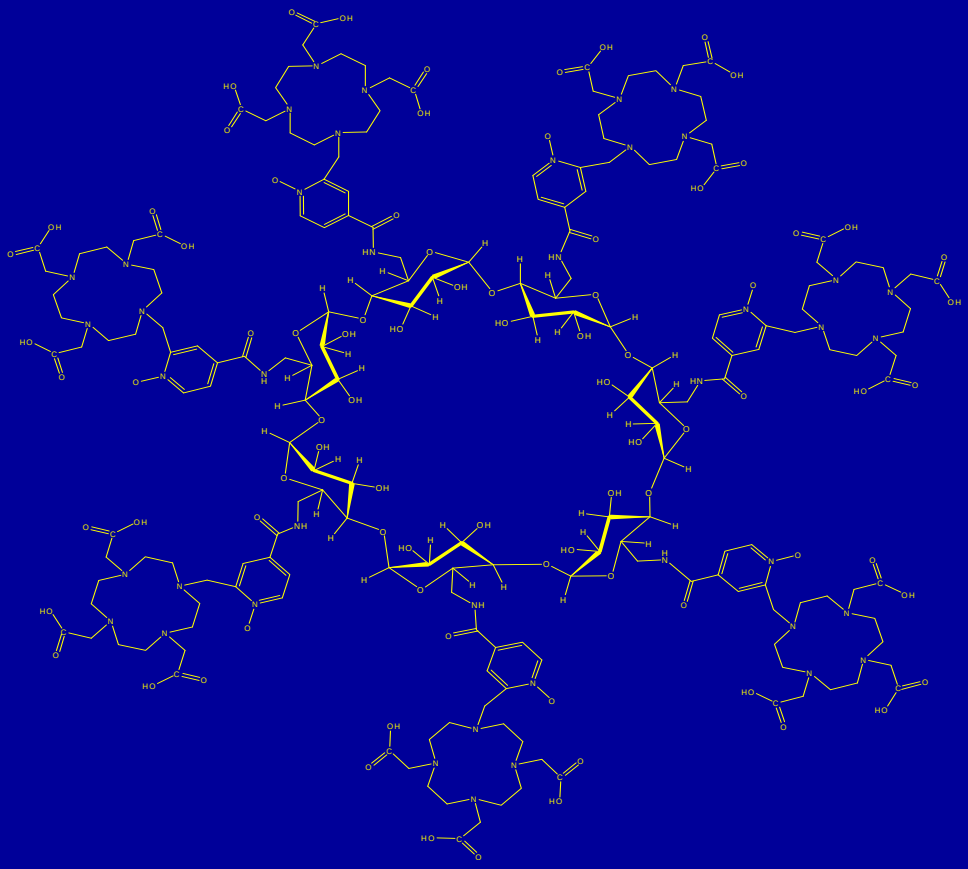

^{1}H NMRD profiles of Gd(III)DO3A-P$^{BnN\{CS\}}$ conjugate with ß-cyclodextrine

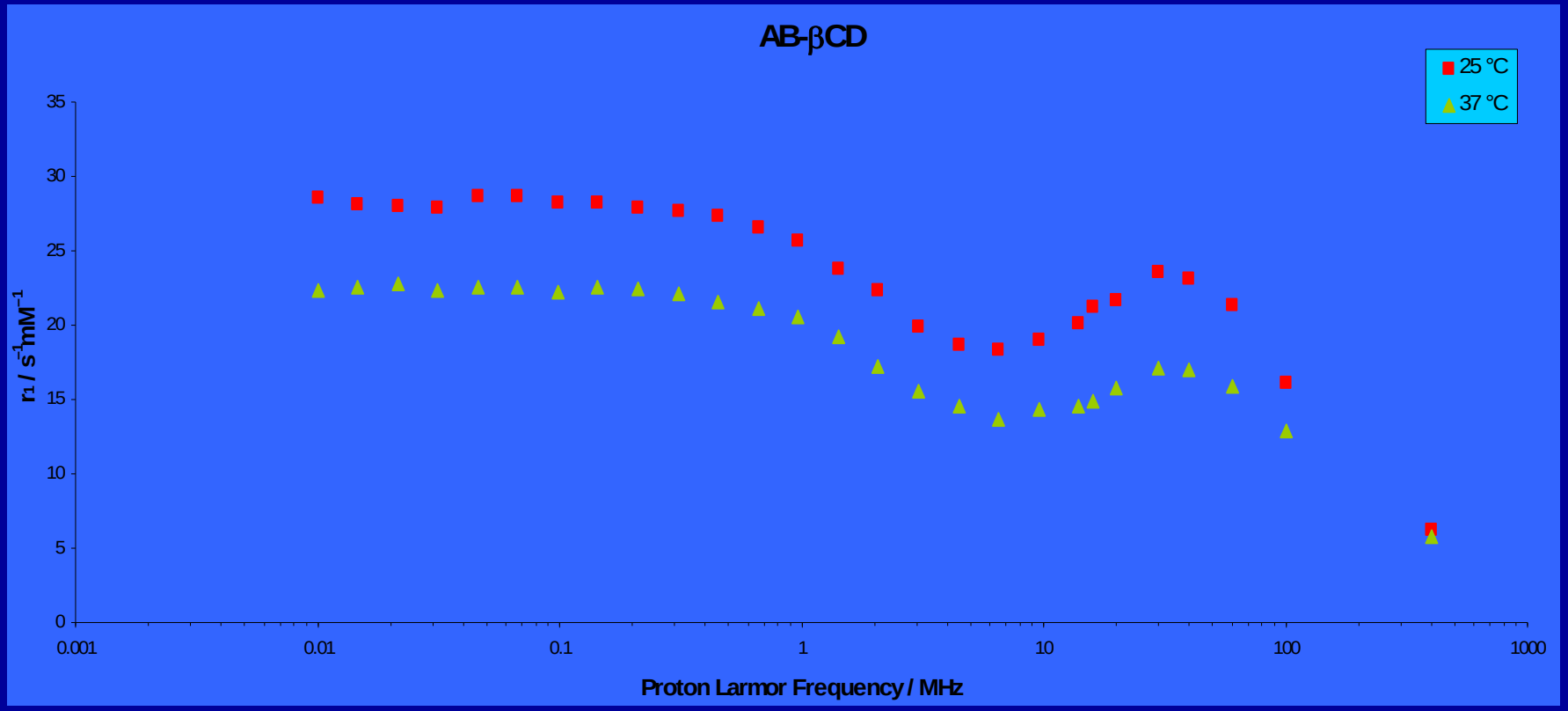

^{1}H NMRD profiles of Gd(III)DO3A-py^{NO-C} conjugate with ß-cyclodextrine

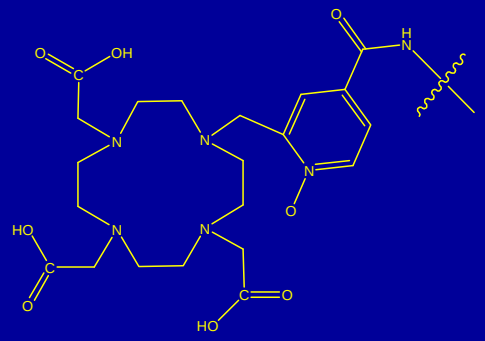

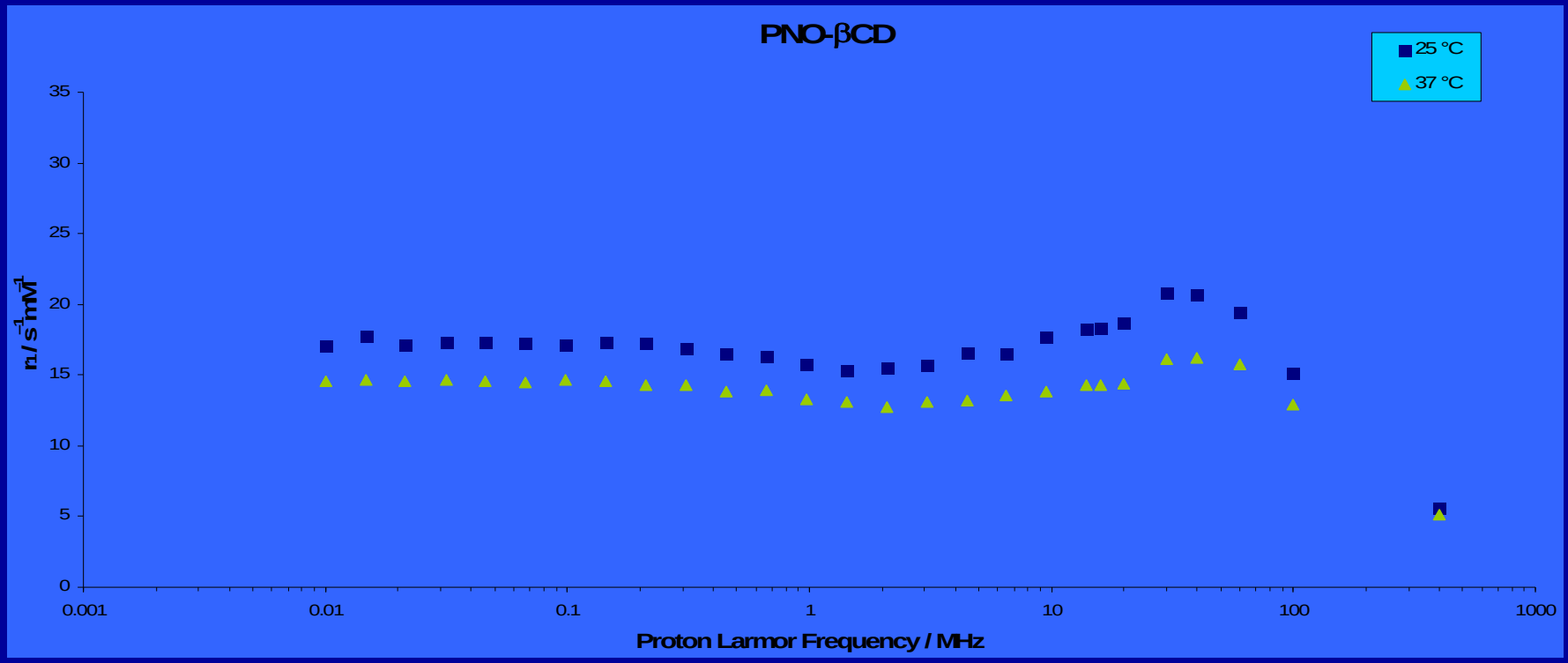

Comparision of PAMAM and CD conjugates

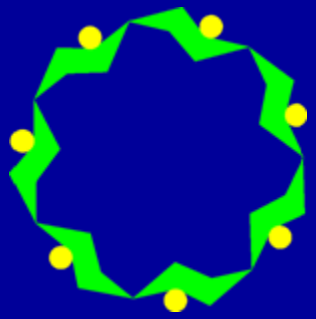

β-cyclodextrine

$r_1(\text{ef.}) = r_1 * N * 1000/M_r$

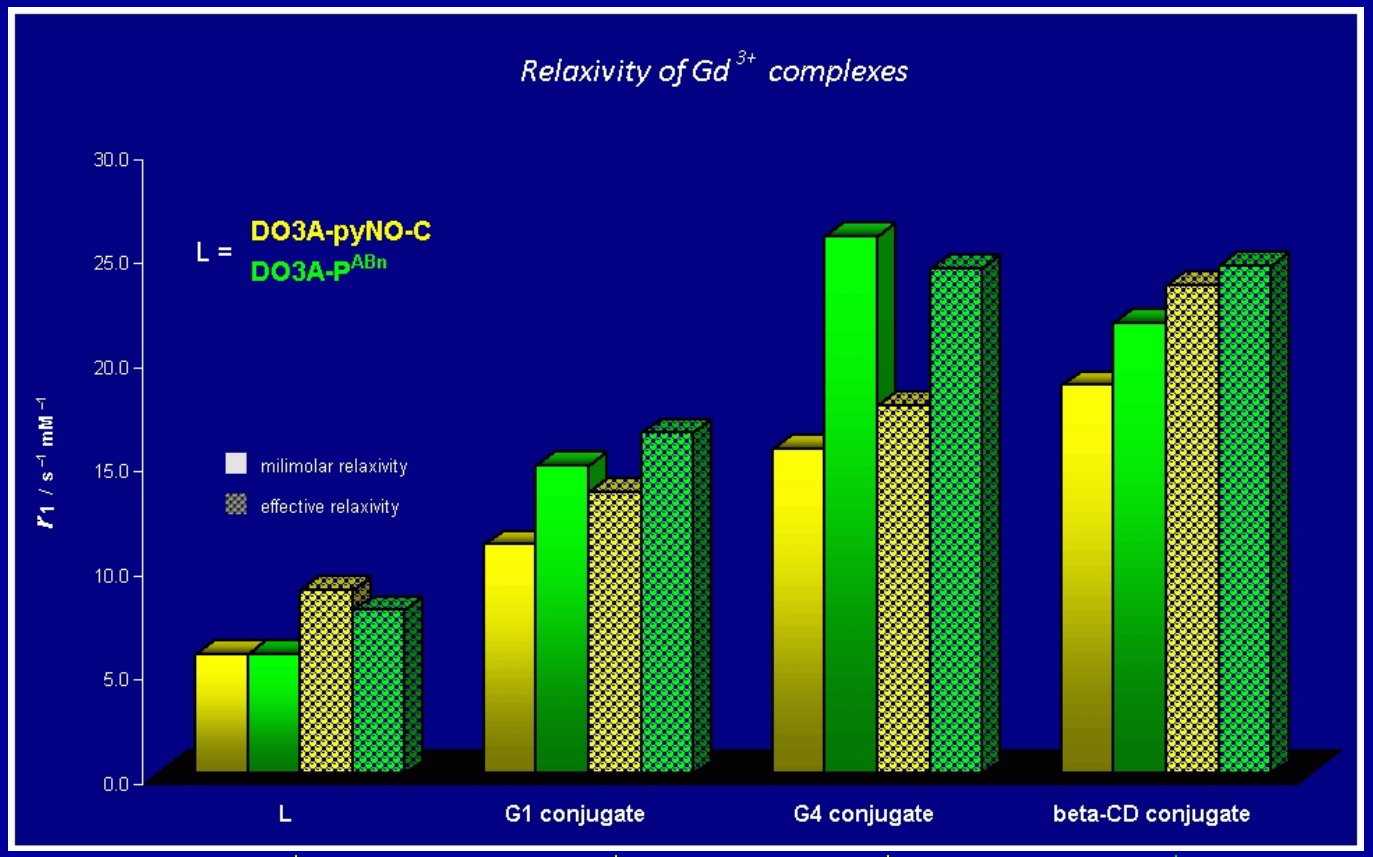

Molecular mass (kDa):	0.6	6.5	50	5.5

Multimodal Probes
Dual Probes

Labelling of Cells

Distribution of the Cells in Organism

Dual Probes

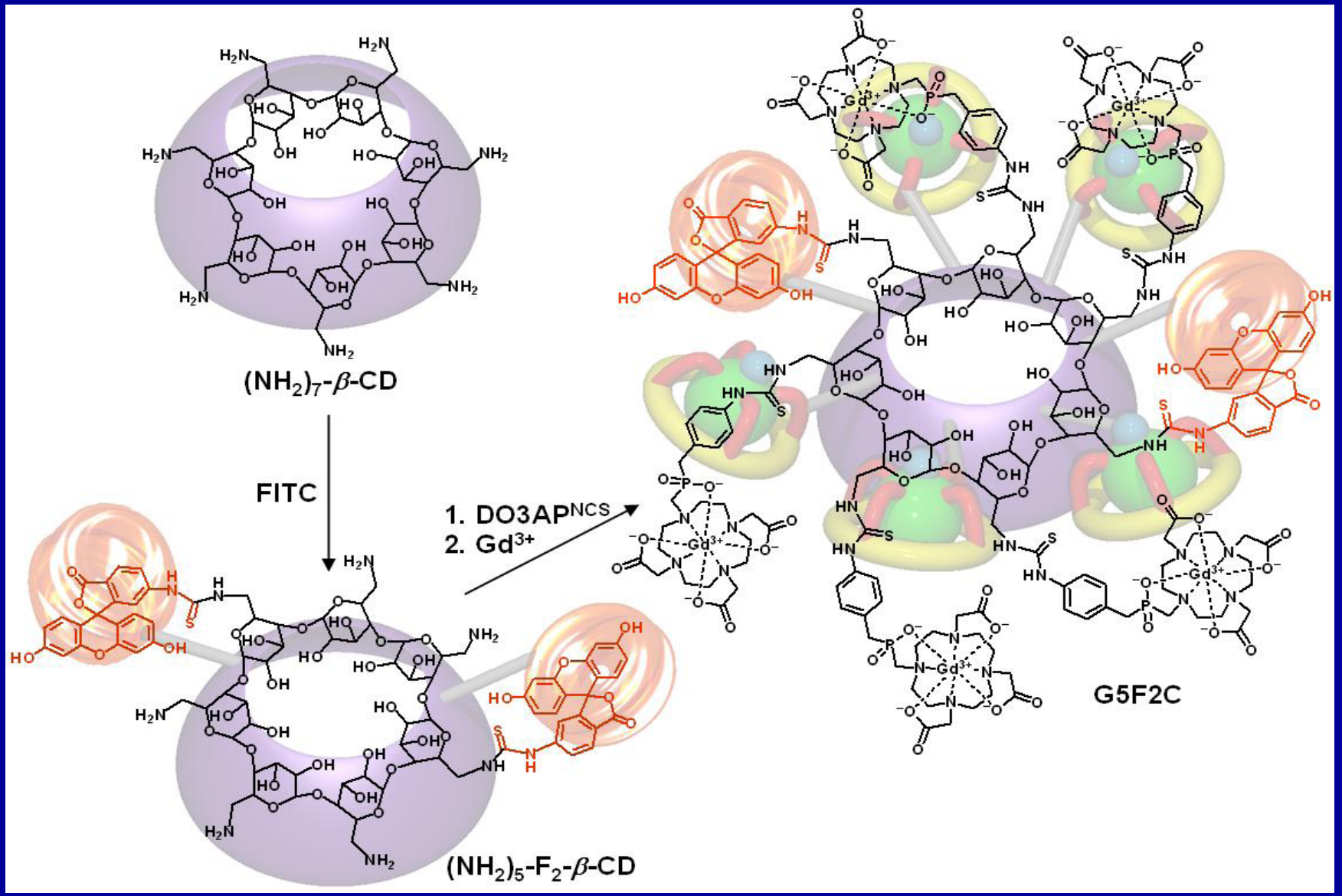

PAMAM dendrimers conjugates

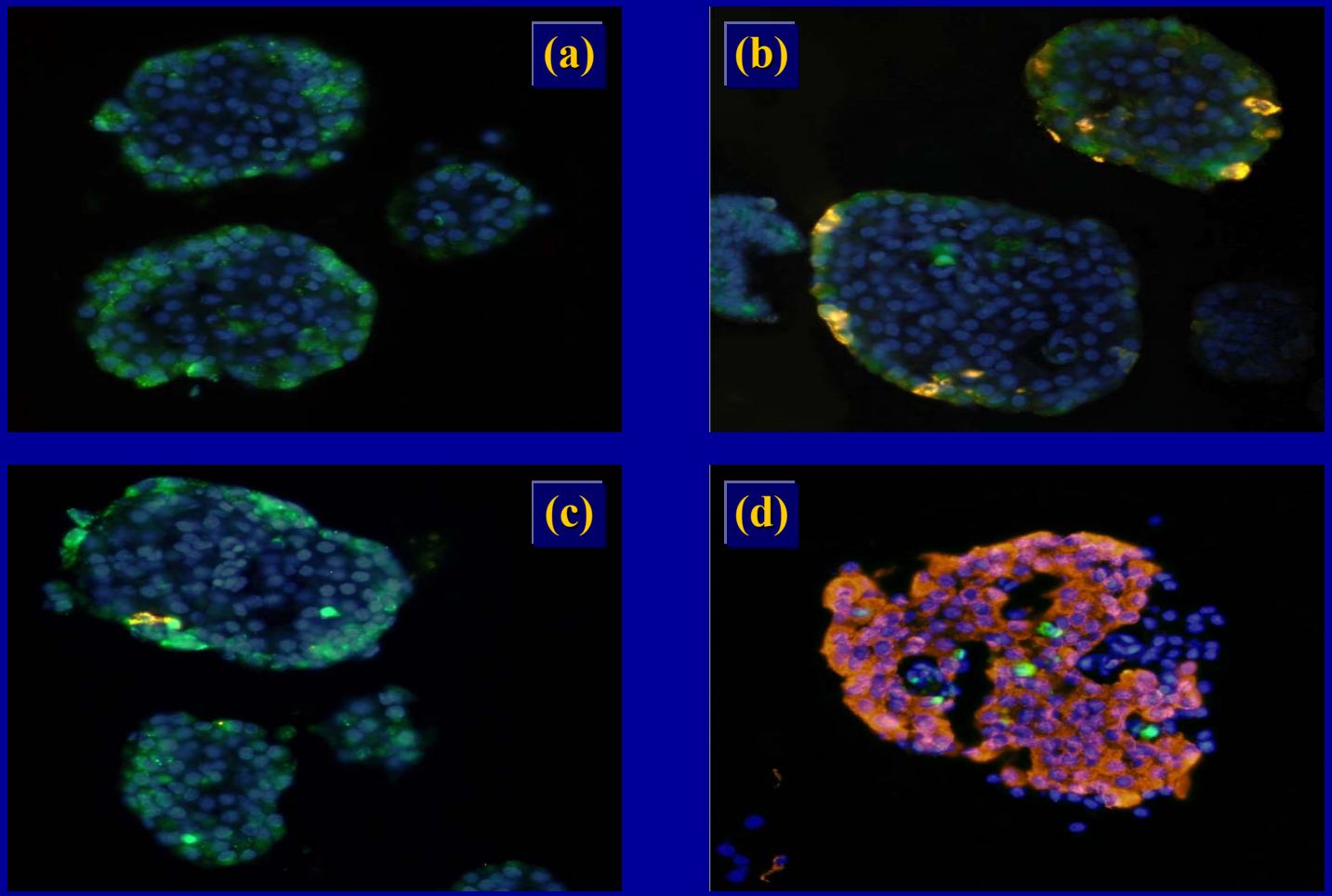

Fluorescent photomicrographs of Langerhans islets labeled by G6.9F0.1C: a) visualization of the contrast agent (green) and karyons (blue); b) highlighting of the a-cells (yellow-orange); c) highlighting of the macrophages (yellow-orange); d) highlighting of the b-cells (pink). Islets were incubated with 1 mm G6.9F0.1C (per Gd^{III}) for 24 h. A typical size of the LIs is 300 μm.

MRI

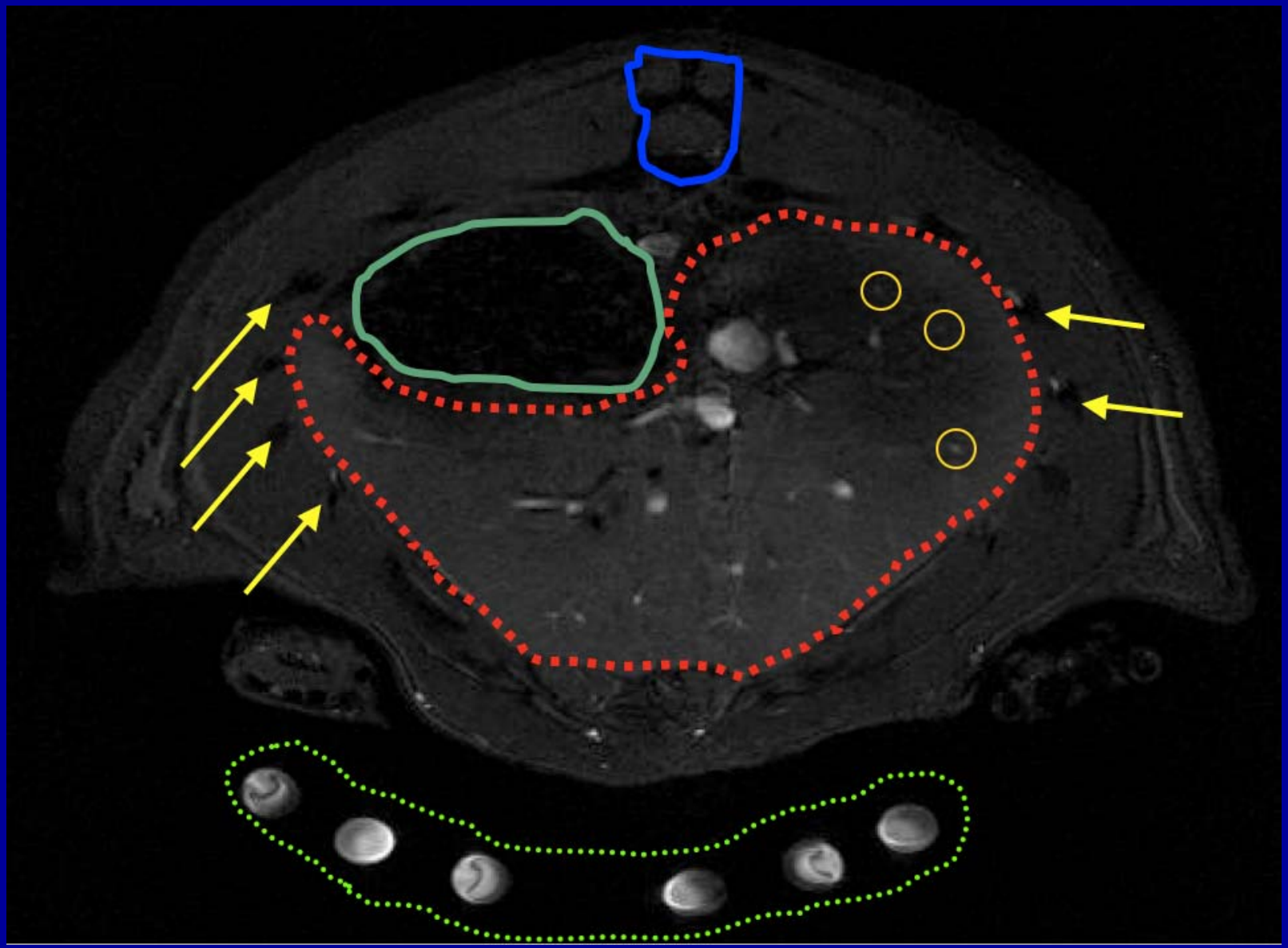

Targeting

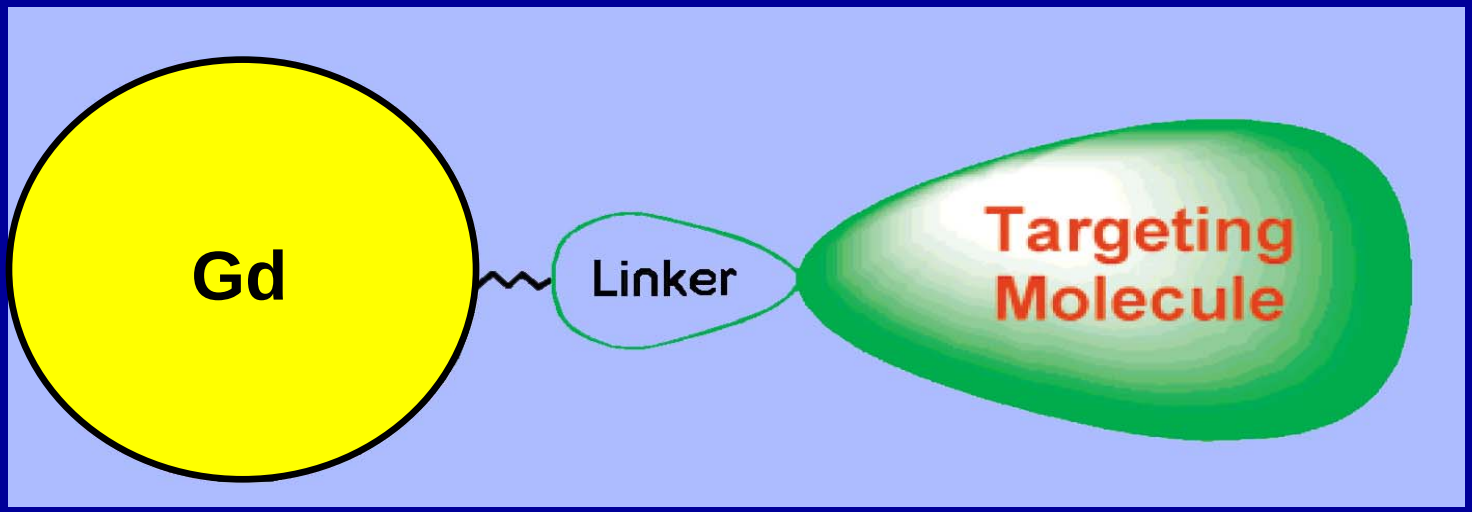

Similar strategy would be applied for development of optical and combined imaging probes.

Relaxometric parameters of Gd(III)–DOTAPP and related ligands

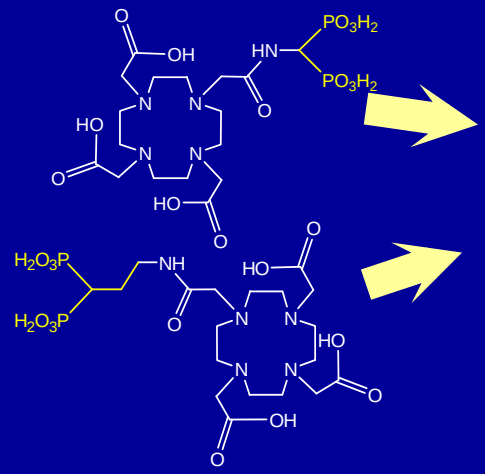

Ligand	Δ^2 [10^{20} s^{-2}]	$^{298}\tau_v$ [ps]	$^{298}\tau_{RH}$ [ps]	$^{298}\tau_M$ [μs]	r_1 [s^{-1} mM^{-1}]
DOTAPP	0.32±0.3	21±1	135±4	1.00±0.08	6.17
BPAMD [a]	0.37	17	88	1.18	5.3
BPAPD [b]	1.22	27	85	1.1	5.0
DOTA [c]	0.16	11	77	0.244	4.8

[a] V. Kubíček, J. Rudovský, J. Kotek, P. Hermann, L. Vander Elst, R. N. Muller, Z. I. Kolar, H. T. Wolterbeek, J. A, Peters, I. Lukeš: *J. Am. Chem. Soc.*, 2005, *127*, 16477–16485.

[b] T. Vitha, V. Kubíček, P. Hermann, L. Vander Elst, R. N. Muller, Z. I. Kolar, H. T. Wolterbeek, W. A. P. Breeman, I. Lukeš, J. A. Peters: *J. Med. Chem.*, 2008, *51*, 677–683.

[c] D. H. Powell, O. M. N. Dhubhghaill, D. Pubanz, L. Helm, Y. S. Lebedev, W. Schlaepfer, A. E. Merbach: *J. Am. Chem. Soc.*, 1996, 118, 9333–9346

Biodistribution

Biodistribution of ^{177}Lu-complexes in Lewis rat 24 h after injection

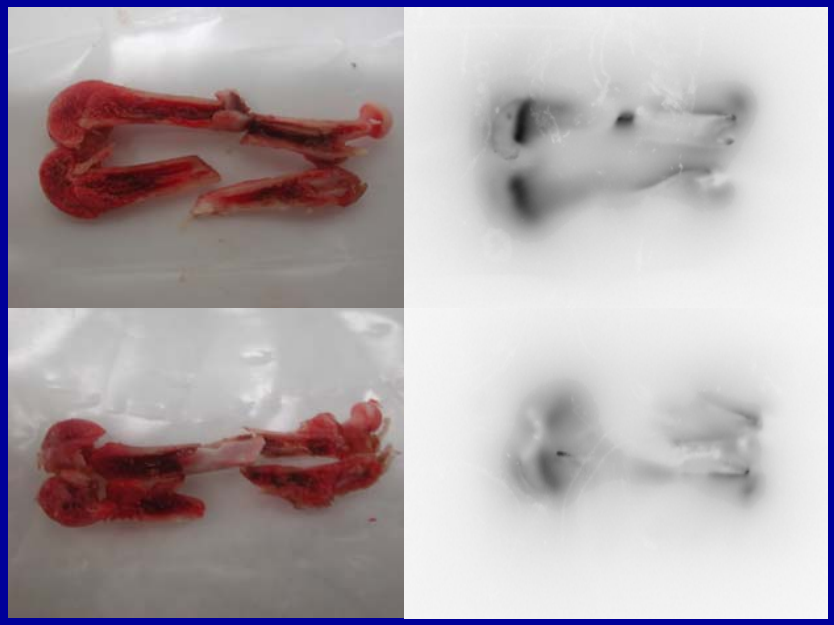

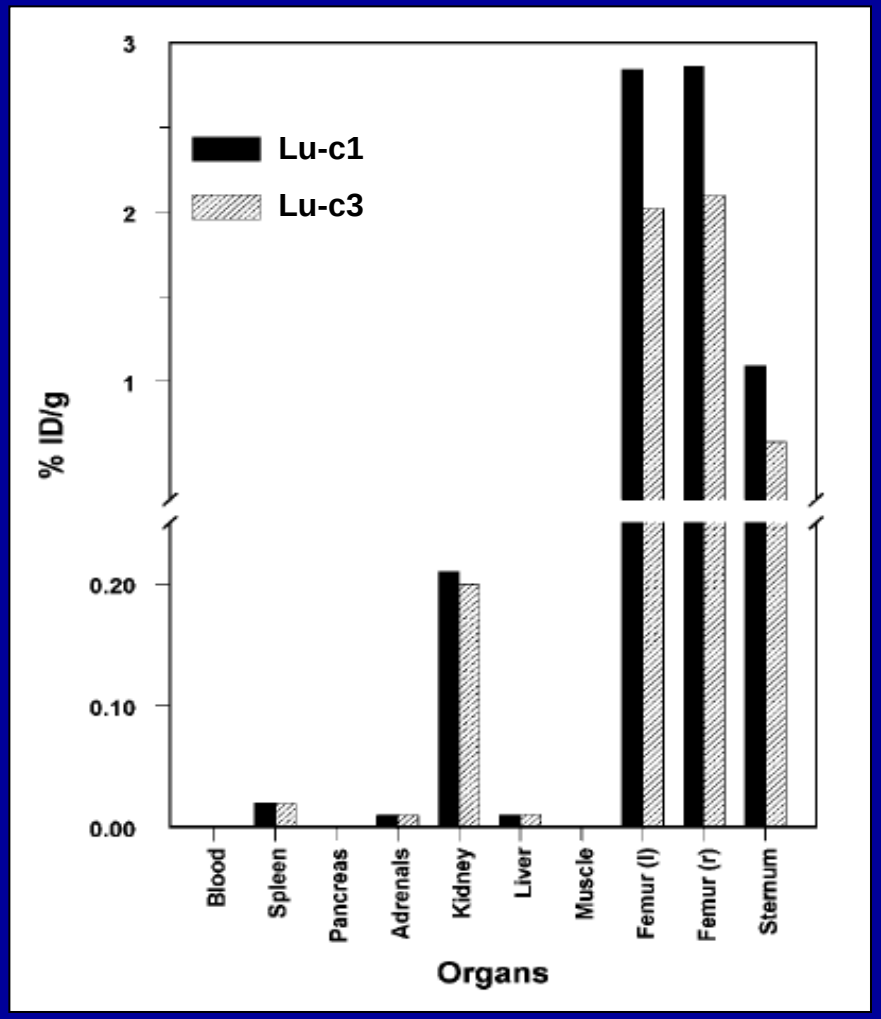

SPECT/CT Imaging of Rats

1 h *p.i.*

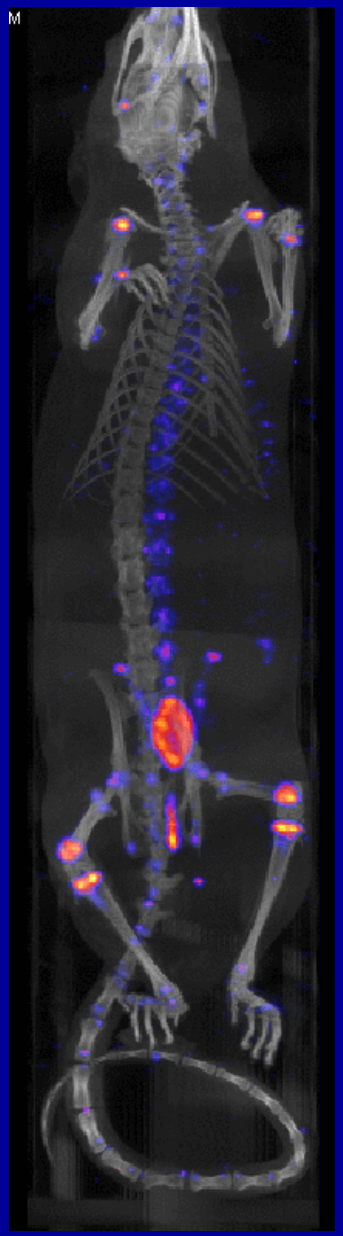

^{177}Lu-c1

75–80 MBq

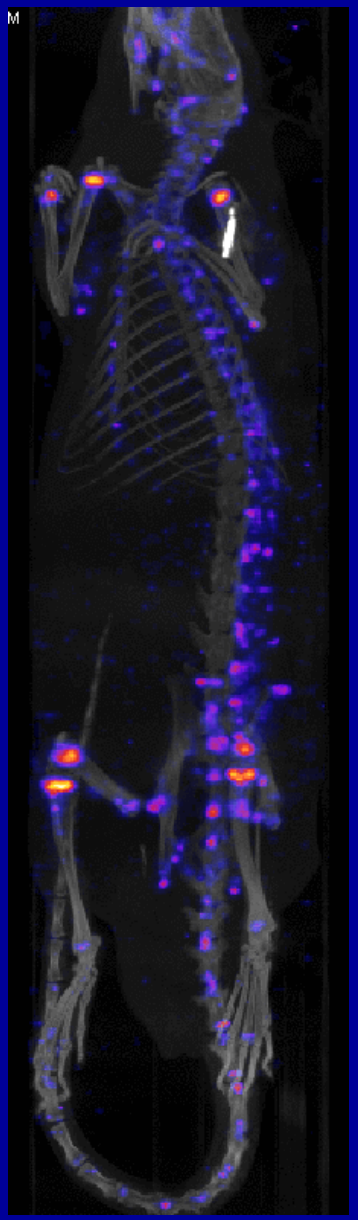

24 h *p.i.*

V. Kubíček, J. Rudovský, J. Kotek, P. Hermann, L. Vander Elst, R. N. Muller, Z. I. Kolar, H. T. Wolterbeek, J. A, Peters, I. Lukeš: *J. Am. Chem. Soc.*, 2005, *127*, 16477–16485.

PET

- ^{18}F (110) min., ^{11}C (20 min.) – cyclotron

Combination of PET and MRI, PET and CT

^{68}Ga (60 min.), generator

Acknowledgements

Support from the Grant Agency of the Czech Republic (No. 203/06/0467), Grant Agency of the Academy of Science of the Czech Republic (No. KAN201110651) and Long-Term Research Plan of the Ministry of Education of the Czech Republic (No. MSM0021620857) are acknowledged. The work was carried out in frame of COST D38 and the EU-supported NoE projects EMIL (No. LSHC-2004-503569) and DiMI (No. LSHB-2005-512146).

Collaboration

Charles University

Doc. Petr Hermann
Dr. Jan Kotek
Dr. Vojtěch Kubíček

Students
Dr. Jakub Rudovský
Zuzana Kotková
Dr. Miloš Polášek
Ivan Řehoř
Dr. Tomáš Vitha

COST D38

Dr. Joop A. Peters (Delft)
Prof. Richard N. Muller (Mons)
Prof. Luce Vander Elst (Mons)
Prof. Lothar Helm (Lausanne)
Prof. Silvio Aime (Torino)
Prof. Mauro Botta (Torino)
Prof. Erno Brücher (Debrecen)
Prof. Carlos F.G.C. Geraldes (Coimbra)
Dr. Eva Toth (Lausanne, Orleans)
Prof. Frank Roesch (Mainz)

IKEM

Dr. Milan Hájek
Dr. Daniel Jirák
Doc. Dr. František Saudek

Institute of Experimental Medicine

Dr. Pavla Jendelová, Prof. Eva Syková